

Loan Only

**CASE FILE
COPY**

**NATIONAL ADVISORY COMMITTEE
FOR AERONAUTICS**

TECHNICAL NOTE 2288

ESTIMATION OF LOW-SPEED LIFT AND HINGE-MOMENT
PARAMETERS FOR FULL-SPAN TRAILING-EDGE
FLAPS ON LIFTING SURFACES WITH AND
WITHOUT SWEEPBACK

By Jules B. Dods, Jr.

Ames Aeronautical Laboratory
Moffett Field, Calif.



Washington

February 1951

Reproduced by
**NATIONAL TECHNICAL
INFORMATION SERVICE**
U S Department of Commerce
Springfield VA 22151

47

NATIONAL ADVISORY COMMITTEE FOR AERONAUTICS

TECHNICAL NOTE 2288

ESTIMATION OF LOW-SPEED LIFT AND HINGE-MOMENT PARAMETERS
FOR FULL-SPAN TRAILING-EDGE FLAPS ON LIFTING SURFACES
WITH AND WITHOUT SWEEPBACK

By Jules B. Dods, Jr.

SUMMARY

Comparisons of the low-speed experimental lift and hinge-moment parameters of flapped lifting surfaces with and without sweepback with values computed by several theoretical procedures are presented. Based on these limited results one theoretical method appears to be more satisfactory than the other methods investigated and is therefore recommended for preliminary design estimates. The method involves adjustments to the section values of the lift and hinge-moment parameters for the effects of induced angle of attack and of induced camber to obtain the values for a finite aspect ratio. The induced angle-of-attack corrections are obtained from the lift-curve slopes calculated by the Weissinger method, and the induced-camber corrections are obtained from an adaptation of the Falkner lifting-surface procedure. Although the method recommended is based upon lifting-surface theory, it may be applied without knowledge of this theory since the necessary information is given in design charts presented herein and in NACA Rep. 921, 1948. Sample calculations are included.

INTRODUCTION

The work of references 1, 2, and 3 has illustrated the advantages of lifting-surface theory over lifting-line theory for estimating the lift and hinge-moment parameters for horizontal-tail surfaces with elevators, or in general, for any lifting surface. The lifting-surface theory given in reference 2 has proved to be superior to the lifting-line theory for the computation of the lift and hinge-moment parameters and is easily used, but this particular method is not applicable to swept-back airfoils.

An attempt to extend the general procedure of lifting-surface theory to swept-back airfoils has been reported in reference 4 wherein the Falkner procedure (references 5 and 6) was used in computing the load distribution. The conclusion reached in reference 4 was that the

hinge-moment parameters computed for swept-back surfaces were in error to such an extent as to invalidate the method. On the basis of the results of reference 4 and subsequent calculations, it has been concluded that the reason for the failure of the method involving a load distribution obtained by the Falkner procedure was the inability to predict the lift-curve slope accurately, and hence the inability to predict the induced angle-of-attack correction to the section parameters for the effects of a finite aspect ratio.

The purpose of the present investigation was to develop a satisfactory method based upon lifting-surface theory for estimating the lift and hinge-moment parameters for swept-back airfoils. The results of experimental information available in reference 7 were used for comparison. The results of the analysis are presented for airfoils having aspect ratios from 2 to 6, and having angles of sweepback up to 45° . Sample calculations are presented for one airfoil.

NOTATION

Coefficients

- C_h flap hinge-moment coefficient $\left(\frac{H}{2qM_A} \right)$
- c_h section flap hinge-moment coefficient $\left(\frac{h}{qc_p^2} \right)$
- C_L lift coefficient $\left(\frac{L}{qS} \right)$
- c_l section lift coefficient $\left(\frac{l}{qc} \right)$

Symbols

- A aspect ratio $\left(\frac{2b^2}{S} \right)$
- $a_{m,n}$ unknown coefficients in Falkner load-distribution series
- b span of the semispan models measured perpendicular to the plane of symmetry, feet
- c chord of the models measured parallel to the plane of symmetry, feet

c' chord of the models measured perpendicular to the sweep reference line of the swept-back models (c' equivalent to c for the unswept models), feet

\bar{c} mean aerodynamic chord $\left(\frac{\int_0^b c^2 dy}{\int_0^b c dy} \right)$, feet

c_f' chord of the flap behind the hinge line, measured perpendicular to the hinge line, feet

H hinge moment, foot-pounds

h section hinge moment, foot-pounds per foot

L lift, pounds

l section lift, pounds per foot

M_A moment about the hinge line of the flap area behind the hinge line, feet cubed

q free-stream dynamic pressure $\left(\frac{1}{2} \rho V^2 \right)$, pounds per square foot

S area of semispan models, square feet

V velocity of air, feet per second

x longitudinal coordinate referred to 0.5c line, feet

y lateral distance, feet

α angle of attack, degrees

α_i average induced angle of attack, degrees

α_o section angle of attack, degrees

δ flap deflection (positive when trailing edge of flap is down) measured in a plane normal to the hinge line, degrees

Λ angle of sweepback of one-quarter-chord line, unless otherwise noted, degrees

λ taper ratio (ratio of tip chord to root chord)

ρ density of air, slugs per cubic foot

θ circular longitudinal coordinate $\left(\cos^{-1} \frac{2x}{c}\right)$

Subscripts

C_L constant lift coefficient
 c_l constant section lift coefficient
 exp experimental
 h flap hinge line
 LS lifting surface
 SC induced camber (streamline curvature)
 $\Lambda=0$ unswept
 Λ swept-back

Parameters

$$C_{h_\alpha} = \left(\frac{\partial C_h}{\partial \alpha}\right)_{\delta=0}; \quad C_{h_{\alpha_0}} = \left(\frac{\partial C_h}{\partial \alpha_0}\right)_{\delta=0} \quad (\text{determined through } \alpha = 0 \text{ or } \alpha_0 = 0), \text{ per degree}$$

$$C_{h_\delta} = \left(\frac{\partial C_h}{\partial \delta}\right)_{\alpha=0}; \quad C_{h_\delta} = \left(\frac{\partial C_h}{\partial \delta}\right)_{\alpha_0=0} \quad (\text{determined through } \delta = 0), \text{ per degree}$$

$$C_{L_\alpha} = \left(\frac{\partial C_L}{\partial \alpha}\right)_{\delta=0}; \quad C_{L_{\alpha_0}} = \left(\frac{\partial C_L}{\partial \alpha_0}\right)_{\delta=0} \quad (\text{determined through } \alpha = 0 \text{ or } \alpha_0 = 0), \text{ per degree}$$

C_{L_α} lift-curve slope computed from the Falkner loading coefficients, $a_{m,n}$, per degree

$$C_{L_\delta} = \left(\frac{\partial C_L}{\partial \delta}\right)_{\alpha=0}; \quad C_{L_\delta} = \left(\frac{\partial C_L}{\partial \delta}\right)_{\alpha_0=0} \quad (\text{determined through } \delta = 0), \text{ per degree}$$

$$(\alpha_\delta)_{C_L} = -\frac{C_{L_\delta}}{C_{L_\alpha}}; \quad (\alpha_\delta)_{c_l} = -\frac{c_{l_\delta}}{c_{l_\alpha}} \quad (\text{flap-effectiveness parameter})$$

THEORETICAL METHODS FOR ESTIMATING THE LIFT AND HINGE-MOMENT PARAMETERS

General Procedure

In computing the values of $C_{L\alpha}$, $C_{L\delta}$, $(\alpha_\delta)_{C_L}$, $C_{h\alpha}$, and $C_{h\delta}$ for a finite-span flapped lifting surface, it is assumed that the corresponding section values $c_{l_{\alpha_0}}$, c_{l_δ} , $(\alpha_\delta)_{c_l}$, $c_{h_{\alpha_0}}$, and c_{h_δ} are known for the particular airfoil section, flap-chord ratio, flap-gap-to-chord ratio, type of flap balance, Mach number, and Reynolds number, or that they can be approximated with reasonable accuracy.¹ These section values are corrected for the effects of induced angle of attack and of induced camber (streamline curvature in the notation of reference 2) to obtain the values for a finite aspect ratio. The equations for the hinge-moment parameters are essentially in the form of the classical lifting-line theory with additive corrections obtained from a particular solution of lifting-surface theory. This general procedure is well known and has been previously established in reference 2 for airfoils without sweep. The evaluation of the induced angle-of-attack effects and of the induced-camber effects presented herein for swept-back airfoils differs considerably, however, from that of reference 2.

The evaluation of the induced angle-of-attack correction is based upon the average reduction in the additional-type loading that occurs between an infinite-span airfoil and an airfoil having a finite span, at a constant angle of attack. The reduction in the additional-type loading is also accompanied by a change in the chordwise distribution of load, which is the induced-camber effect. This effect is evaluated by a spanwise integration of the resulting change in the hinge moment at each section of the control surface.

The many variables encountered in the aerodynamic design of a flapped lifting surface make it difficult to obtain a generalized solution. Thus, the theoretical results presented herein are limited (1) to the range wherein the variation of the hinge-moment coefficients with angle of attack and with flap deflection is linear; (2) to constant-percent-chord flaps extending over the full span of the lifting surface; (3) to flaps having internally sealed radius noses; and (4) to low

¹In the absence of experimental section data that correspond exactly to the design conditions, approximations to the section data may be made from available section data by the methods of reference 8.

subsonic speeds.² It is also assumed that the airfoil profiles and the flap-chord ratios of the finite-span and the infinite-span airfoils are identical in planes perpendicular to the quarter-chord lines.

Application of the General Procedure to Specific Methods

The application of the general procedures for evaluating the effects of finite aspect ratio on the section parameters will now be discussed in regard to the individual methods presented. The theoretical results obtained by each method are compared with the experimental results in figures 1 through 9. A discussion of the correlation of the theoretical results obtained by each method with the experimental results is deferred to a later section.

Application to method 1.—Method 1 is a modified version of the procedure used in reference 4. The evaluation of the average induced angle-of-attack and the induced-camber corrections for the effects of finite aspect ratio presented in reference 4 was accomplished by applying the results of a Falkner lifting-surface solution to the computation of the lift and hinge-moment parameters. This procedure resulted in an unsatisfactory agreement with the experimental results then available for the models having aspect ratios of 3.0 and 4.5, particularly for those models having sweepback. Subsequently, additional experimental results became available for models with and without sweep having aspect ratios of 2 and 6. Computations made by the same procedure showed equally poor correlation with the experimental results for these models.

Method 1 is an attempt to improve the agreement between theory and experiment for the swept-back models. It is not as rigorous as the method of reference 4 in that the section lift-curve slopes are reduced according to the simplified theory for the effects of sweep. The resulting smaller induced angle-of-attack effects are then applied to the remaining section parameters $c_{l\delta}$, $c_{h\alpha}$, and $c_{h\delta}$ which have also been reduced by their proper $\cos \Lambda$ function to obtain the parameters for a finite aspect ratio. Although this method gave somewhat better agreement than that of reference 4, it is not recommended for use. It is included to aid in the development of method 2, and as a note of caution in the use of method 1. The details of the application of the method and sample calculations are given in the appendix. The results of the calculations are presented in figure 1.

Application to method 2.—On the basis of the results presented in reference 4, and the modification of the procedure as presented under

²First-order compressibility effects may be taken into account by application of the Prandtl-Glauert rule. (See p. 10, reference 2.)

method 1, it has been concluded that the main reason for the failure of the Falkner procedure was the inability to predict the lift-curve slope accurately, even by using the sweep corrections to the section lift-curve slope, and hence the inability to predict accurately the induced angle-of-attack corrections to the section parameters for the effects of finite aspect ratio. However, it will be shown that the Falkner method gives accurate values of the induced-camber correction to the rate of change of the hinge-moment coefficient with angle of attack $\left(\Delta C_{h\alpha}\right)_{SC}$,

indicating that the chordwise boundary conditions are satisfied with sufficient accuracy. A logical development based on these facts then appeared to be to find an accurate method for predicting the induced angle-of-attack effects to be used with the induced-camber effects computed from the Falkner loading. It was found that the method of J. Weissinger, as reported in reference 9, gave the best correlation of the theoretical lift-curve slopes with the experimental lift-curve slopes, and hence, the best values of the induced angle-of-attack corrections. Thus, method 2 consists of a combination of these two procedures.

A question concerning the advisability of using the induced-camber correction to $C_{h\alpha}$ as computed from the Falkner loading coefficients arises in view of the fact that the lift-curve slope is not accurately computed from these same loading coefficients. It is believed that the answer to this question lies in the fact that the induced-camber correction to $C_{h\alpha}$ is primarily a function of the chordwise distribution of the load and secondarily, of the absolute value of the lift. Inasmuch as the Falkner method satisfies the chordwise boundary conditions with sufficient accuracy, it enables an accurate prediction of the induced-camber correction to be made. Supporting evidence is offered

in figure 10 wherein the values of $\left(\Delta C_{h\alpha}\right)_{SC}$ computed by the Falkner

method and the method of references 2 and 10 are compared with a pseudo-experimental value

$$\left[\left(\Delta C_{h\alpha}\right)_{SC}\right]_{exp} = \left(C_{h\alpha}\right)_{exp} - \left[\left(C_{h\alpha_0}\right)_{\Lambda=0}\right]_{exp} (\cos \Lambda) \left(1 - \frac{\alpha_1}{\alpha}\right)_{exp}$$

The term $\left[\left(\Delta C_{h\alpha}\right)_{SC}\right]_{exp}$ is called a pseudo-experimental value

because it is impossible to measure it experimentally by direct means. However, the remaining factors in the above equation can be measured

experimentally, enabling the determination of $\left[\left(\Delta C_{h\alpha}\right)_{SC}\right]_{exp}$. The results presented in figure 10 show that much better agreement with the pseudo-experimental values of $\left(\Delta C_{h\alpha}\right)_{SC}$ is obtained by the Falkner

theory³ (method 1) than by the theory of references 2 and 10 (method 4), especially for models having large angles of sweepback.

Since the computation of the induced-camber correction to $C_{h\alpha}$ by the Falkner method is rather involved, design charts (figs. 11 and 12) are presented so that these values may be determined directly for flap-chord ratios from 0.20 to 0.40, for aspect ratios from 2 to 6, and for airfoils having up to 45° of sweepback. It should be noted that the flap-chord ratios for the swept-back models were taken in the plane perpendicular to the 0.25-chord line. (If the values of $\left(\Delta C_{h\alpha}\right)_{SC}$ are desired using the flap-chord ratio measured in the plane of symmetry, the equivalent ratio perpendicular to the 0.25-chord line should be computed and used in the charts.)

The application of the method is presented in detail in the appendix. The results obtained by this procedure are presented in figure 2.

Application to method 3.— This method combines the induced angle-of-attack corrections of method 2 with the induced-camber correction to $C_{h\alpha}$ and $C_{h\delta}$ as given in reference 10. The results of the computation by this method are given in figure 3. The purpose in presenting this method is to show that the induced-camber correction to $C_{h\alpha}$ given in reference 10 is not satisfactory, as is evident from a comparison of figures 2 and 3. From figure 10 it can be seen that the procedure of reference 10, intended only as a rough approximation for correcting the values of $\left(\Delta C_{h\alpha}\right)_{SC}$ for unswept airfoils by $\cos \Lambda$ to find the corresponding values for swept-back airfoils, results in values which vary considerably from those determined by lifting-surface theory.

Application to method 4.— This method is an approximate way of accounting for the effects of sweep by applying modified lifting-line theory to the equations for the hinge-moment parameters of unswept airfoils. The application of this method is explained in reference 10. It is recommended therein only for rough approximation. Although no emphasis was placed upon the computation of $C_{L\delta}$ in reference 10, values of $C_{L\delta}$ which were computed by the relationship $C_{L\delta} = \left[\left(\alpha_\delta \right) c_l \right]_{\Lambda=0} \cos \Lambda_h$ are included herein for completeness. (See fig. 4.)

Application to method 5.— The application of this lifting-surface method to airfoils without sweepback is fully explained in reference 2. (See fig. 5.)

³Swanson's empirical viscosity factor η has been used in computing $\left(\Delta C_{h\alpha}\right)_{SC}$ by the Falkner method.

DESCRIPTION OF EXPERIMENTAL MODELS AND TESTS

Models

The semispan, reflection-plane, model horizontal tails reported in reference 7 had a taper ratio (ratio of tip chord to root chord) of 0.5 and aspect ratios of 2, 3, 4.5, and 6. The geometry of the models is shown in table I.

The angles of sweepback of the quarter-chord lines, which are used as the sweep reference lines, were 16.7° , 11.3° , 7.6° , and 5.7° for the models having aspect ratios of 2, 3, 4.5, and 6, respectively, and having the hinge lines without sweep. These models are referred to throughout the report as the unswept models although the sweep reference lines had some sweepback. For the unswept models the NACA 64A010 airfoil sections were parallel to the plane of symmetry.

The swept-back models, which had the same aspect ratios as the unswept models, had either 35° or 45° sweepback. For these models the sweep reference line is that line which joins the 0.25-chord points of the NACA 64A010 airfoil sections, which were inclined to the plane of symmetry at an angle equal to the angle of sweepback.

The choice of these sweep reference lines was dictated by considerations of the simplified theory for the effects of sweep. According to this theory, the finite-span and the infinite-span models should have identical airfoil sections and flap-chord ratios in planes perpendicular to the quarter-chord lines. Therefore, the swept-back models were constructed in this manner. To be strictly consistent, the unswept models should have been constructed in the same manner, but since the angles of sweepback were small, differences incurred by placing the airfoil profile and the 0.30 flap-chord ratio parallel to the plane of symmetry are negligible.

All models were equipped with sealed, radius-nose, full-span flaps. The gaps between the flaps and the shrouds and the gaps between the flap noses and the plates in the balance chamber (seal gap) are shown in table I, section B-B. Flap-nose gaps were sealed over the complete span of the models, and end seals were provided at the reflection plane and at the outboard hinge brackets, which were at 82 percent of the span. The inboard hinge brackets were immediately below the tunnel floor. It was necessary to place an additional sealed hinge bracket at 38 percent of the semispan for the model having an aspect ratio of 6 with 35° of sweepback.

The tip shapes were formed by rotating the airfoil section about a line inboard of the tip a distance equal to one-half the maximum thickness of the tip airfoil section.

Tests to obtain the basic section (or infinite span) data were made with a two-dimensional model having a chord of 3.5 feet and having the NACA 64A010 section parallel to the undisturbed air stream. The flap-chord ratio was 0.30.

Tests

Most of the experimental lift and hinge-moment parameters used in this report were obtained from tests of the afore-mentioned models conducted in the Ames 7- by 10-foot wind tunnels and reported in reference 7. These parameters were for a Reynolds number of 3 million based upon the mean aerodynamic chords. The Mach numbers were approximately 0.20 for all the models. The test results for the model of aspect ratio 3 having 45° of sweepback were obtained from the Ames 12-foot pressure wind tunnel for the same Reynolds number and for about the same Mach number. The lift of the models was measured by means of the wind-tunnel balance systems, and the flap hinge moments were measured by means of resistance-type torsional strain gages. All coefficients and the angle of attack were corrected for the interference effects of the tunnel walls.

CORRELATION OF THEORETICAL AND EXPERIMENTAL RESULTS

The results of the theoretical and experimental investigation are presented for the lift and hinge-moment parameters (1) as a function of the aspect ratio for various amounts of sweepback in figures 1 to 5, and (2) as a function of the angle of sweepback for various aspect ratios in figures 6 through 9. The numerical values are summarized for the foregoing results in table II. The sample calculations are given in the appendix for methods 1 and 2.

Correlation of Method 1 With Experiment

The application of cosine corrections to the section parameters for the effects of sweepback resulted in much better correlation of the calculated parameters with the experimental parameters for the swept-back models than did the Falkner method as applied in reference 4. However, the computed values of the lift-curve slopes of the unswept models still were consistently high throughout the aspect-ratio range from 2 to 6 investigated herein. In general, the correlation with experiment (fig. 1) is not as satisfactory as that obtained for method 2 (fig. 2), particularly for the values of $C_{h\alpha}$ and $C_{h\delta}$ for the unswept models. Since the same induced-camber corrections are used for both method 1 and method 2, the poorer agreement of method 1 with the experimental values must be due to errors in the induced angle-of-attack correction.

Correlation of Method 2 With Experiment

In general, the correlation of method 2 with experiment shown in figure 2 is considered to be better than that obtained by the other methods investigated herein, and, therefore, method 2 is recommended for preliminary design estimates. This recommendation is based on consideration of the lift as well as the hinge-moment parameters for airfoils with and without sweepback. This procedure is not superior to the other methods investigated for each parameter for all angles of sweepback and for all aspect ratios. It is believed, however, that because of the more generally correct variation of the parameters with sweepback and aspect ratio, this method will result usually in more acceptable preliminary design estimates. The largest error involved in the estimation of $C_{h\alpha}$ is of the order of magnitude of 0.0008 for the 35° swept-back models, which is a reasonably small error considering that the average error previously encountered even for unswept horizontal tails is of about the same magnitude. (See table I of references 2 and 8.) The maximum error for the values of $C_{h\alpha}$ for either the unswept models, or the two 45° swept-back models does not exceed 0.0003, a value not much in excess of the experimental accuracy. Although the predicted values of $C_{h\alpha}$ for the 35° swept-back models for both methods 3 and 4 are nearer the experimental values, it is believed to be merely a fortuitous condition since the incorrect variation of $C_{h\alpha}$ with sweepback given by these methods results in considerably less accurate results for both the unswept models and the models swept back 45° .

The accuracy of the theoretical predictions of $C_{h\delta}$ and $C_{L\alpha}$ by method 2 is better than for any of the other methods. (The values of $C_{L\alpha}$ are identical for methods 2 and 3.) The accuracy of the predictions of $C_{L\delta}$ for the unswept models is not as good for method 2 as for method 1, 4, or 5, but method 2 is superior to any method investigated for predicting $C_{L\delta}$ for the swept-back models for the sweep range considered

herein. It should be noted that the value of $\left[\left(\alpha_\delta \right)_{c_l} \right]_{\Lambda=0} \cos \Lambda$ is in

error because the effect of sweep is underestimated by this method between the unswept models and the models swept back 35° , while the effect of sweep is overestimated between the models swept back 35° and those swept back 45° . A part of the errors in estimating $C_{L\delta}$ must, of course, be attributed to the small errors in estimating $C_{L\alpha}$.

Correlation of Method 3 With Experiment

The correlation of method 3 with experiment is shown in figure 3. A comparison of the results obtained by this method with the results

obtained by method 2 illustrates the large effect of the induced-camber correction to $C_{h\alpha}$ on the hinge-moment parameters since the same induced angle-of-attack corrections were used for both methods. The variation of $C_{h\alpha}$ (fig. 3) with increasing sweepback is in the wrong direction. The values of $C_{h\delta}$ are in fair agreement with the experimental values, but are not as close as those of method 2.

Correlation of Method 4 With Experiment

The correlation of method 4 with experiment is shown in figure 4. As in the preceding method, the induced-camber correction to $C_{h\alpha}$ results in a variation of $C_{h\alpha}$ with increasing sweepback which is in the wrong direction. Although the computed values of $C_{h\alpha}$ for the 35° swept-back models agree well with the experimental values, the agreement obtained for the unswept models and for the models swept back 45° is not as good as that obtained by method 2. The correlation of the rate of change of hinge-moment coefficient with flap deflection $C_{h\delta}$ obtained for the models both with and without sweepback is likewise not as good as that given by method 2. The values of $C_{L\delta}$ agree reasonably well because of compensating errors in $\left[\left(\alpha_\delta \right)_{c_l} \right]_{\Lambda=0} \cos \Lambda_h$ and $C_{L\alpha}$.

Correlation of Method 5 With Experiment

This method is a lifting-surface procedure applicable only to airfoils without sweepback and is presented in reference 2. The method recommended in the present report gives a slightly better correlation with experiment, except for $C_{L\delta}$ (figs. 2 and 5).

CONCLUDING REMARKS

The experimentally measured low-speed lift and hinge-moment characteristics of various unswept and swept-back flapped lifting surfaces were compared to those predicted by the use of several theoretical procedures. On the basis of these limited results, a method (method 2) is proposed for preliminary design estimates of the low-speed lift and hinge-moment parameters of lifting surfaces having full-span trailing-edge flaps. The method is based upon lift predictions made by the

Weissinger method, which are presented in NACA Rep. 921, 1948, and upon estimates of the induced-camber aspect-ratio corrections to the hinge-moment parameters computed from a lifting-surface solution by the Falkner method. Design charts for the induced-camber correction are provided so that the method may be applied without extensive lifting-surface computations.

Ames Aeronautical Laboratory,
National Advisory Committee for Aeronautics,
Moffett Field, Calif., Apr. 4, 1950.

APPENDIX

SAMPLE CALCULATIONS

The computation of the lift and hinge-moment parameters by methods 1 and 2 is presented for the model having an aspect ratio of 4.5 and swept back 45° . The section characteristics of an NACA 64A010 airfoil having a 0.30-chord flap which were used for all the methods are:

$$c_{l_{\alpha_0}} = 0.108$$

$$c_{l_{\delta}} = 0.065$$

$$(\alpha_{\delta})_{c_l} = -0.60$$

$$c_{h_{\alpha_0}} = -0.0057$$

$$c_{h_{\delta}} = -0.0114$$

Method 1

The computation of the lift-curve slope by the Falkner procedure necessitates a solution for the Falkner loading coefficients. This procedure is explained in detail and computing forms are given in reference 6. From equation (A19), reference 6, expressing $C_{L_{\alpha}}$ per degree

$$C_{L_{\alpha}}' = \frac{A\pi^2}{(16)(57.296)} \left(16a_{0,0} + 8a_{1,0} + 4a_{0,2} + 2a_{1,2} + 2a_{0,4} + a_{1,4} \right)$$

$$C_{L_{\alpha}}' = \frac{2.7758}{57.296} \left[16(0.067684) + 8(0.008287) + 4(0.038488) + 2(-0.024597) + \right.$$

$$\left. 2(0.075509) + (-0.115072) \right]$$

$$= 0.0625$$

This lift-curve slope $C_{L\alpha}'$ is used to determine α_1/C_L and $\frac{(\Delta C_L)_{SC}}{C_L}$. The final lift-curve slope is then found from the following modification of equation (3) of reference 4

$$C_{L\alpha} = \frac{\left(c_{l\alpha_0}\right)_{\Lambda=0} \cos \Lambda}{1 + \left(\frac{\alpha_1}{C_L}\right) \left(c_{l\alpha_0}\right)_{\Lambda=0} \cos \Lambda + \frac{(\Delta C_L)_{SC}}{C_L}}$$

where

$$\frac{(\Delta C_L)_{SC}}{C_L} = \frac{-(\Delta C_L)_{SC}}{\alpha} \left(\frac{1}{C_{L\alpha}'} \right)$$

The following equation, which was based on an integration of the induced-camber load on the control surface, was used to determine

$\frac{(\Delta C_L)_{SC}}{\alpha}$ in reference 4, but was not included therein:

$$\begin{aligned} \frac{(\Delta C_L)_{SC}}{\alpha} &= \frac{A\pi^2}{(16)(57.296)} \left(8a_{1,0} + 2a_{1,2} + a_{1,4} \right) \\ &= \frac{2.7758}{57.296} \left[8(0.008287) + 2(-0.024597) + (-0.115072) \right] \\ &= -0.00475 \end{aligned}$$

Then

$$\frac{(\Delta C_L)_{SC}}{C_L} = \frac{-(-0.00475)}{0.0625} = 0.0760$$

To evaluate $\frac{\alpha_1}{C_L}$, from reference 4,

$$\begin{aligned} \frac{\alpha_1}{C_L} &= 57.296 \left[\frac{1}{C_{L\alpha}'(57.3)} - \frac{1}{2\pi} - \frac{(\Delta C_L)_{SC}}{C_L} \left(\frac{1}{2\pi} \right) \right] \\ &= 57.296 \left[\frac{1}{3.581} - 0.1592 - (0.0760)(0.1592) \right] \\ &= 6.188 \end{aligned}$$

It should be noted that this procedure for evaluating α_1/C_L is somewhat arbitrary because α_1/C_L is evaluated without a sweep correction to the lift-curve slope, that is, in the same manner as reference 4. Calculations made with this correction applied both to α_1/C_L and to C_{L_α} indicated much poorer correlation with the experimental values than the procedure shown here. Substituting the preceding values of $\frac{(\Delta C_L)_{SC}}{C_L}$ and α_1/C_L in the equation for C_{L_α} gives

$$C_{L_\alpha} = \frac{(0.108)(0.707)}{1 + (6.188)(0.108)(0.707) + 0.0760}$$

$$= 0.0493$$

Similarly, the equation of reference 4 for C_{L_δ} becomes

$$C_{L_\delta} = \left(c_{l_\delta} \right)_{\Lambda=0} \cos \Lambda \cos \Lambda_h \left(1 - \frac{\alpha_1}{\alpha} \right) - \left[\left(\alpha_\delta \right) c_l \right]_{\Lambda=0} \cos \Lambda_h \frac{(\Delta C_L)_{SC}}{\alpha}$$

The use of $\cos \Lambda \cos \Lambda_h$ instead of $\cos^2 \Lambda$, and of $\cos \Lambda_h$ instead of $\cos \Lambda$, is an approximation suggested in reference 10 to account for the effects of taper by considering the effective change in the flap deflection to be a function of the sweep of the hinge line rather than

the sweep of the quarter-chord line. To evaluate $\left(1 - \frac{\alpha_1}{\alpha} \right)$ for use in the preceding equation

$$\frac{\alpha_1}{\alpha} = \frac{\alpha_1}{C_L} \left(C_{L_\alpha} \right)$$

$$= (6.188)(0.0493)$$

$$= 0.3051$$

and

$$\left(1 - \frac{\alpha_1}{\alpha} \right) = 0.6949$$

Then

$$C_{L_\delta} = (0.065)(0.5344)(0.6949) - (-0.60)(0.756)(-0.00475)$$

$$= 0.022$$

So that

$$\begin{aligned} \left(\alpha_{\delta} \right)_{c_L} &= - \frac{c_{L\delta}}{c_{L\alpha}} = - \frac{0.022}{0.049} \\ &= -0.449 \end{aligned}$$

Equation (1) of reference 4 becomes

$$\left(c_{h\alpha} \right)_{LS} = \left(c_{h\alpha_0} \right)_{\Lambda=0} \cos \Lambda \left(1 - \frac{\alpha_1}{\alpha} \right) + \left(\Delta c_{h\alpha} \right)_{SC}$$

The evaluation of the induced-camber correction $\left(\Delta c_{h\alpha} \right)_{SC}$ for the effects of finite aspect ratio was obtained from a spanwise and chordwise integration over the flap of the chordwise change in loading attributable to the induced camber. This procedure is based on the assumption that the chordwise distribution of load was of the type given by Falkner $(\cot \theta/2, \sin \theta, \sin 2\theta \dots)$, where $\sin \theta$ and $\sin 2\theta \dots$ are the induced-camber terms. In order to compute the actual values of the induced-camber correction $\left(\Delta c_{h\alpha} \right)_{SC}$ it was necessary to solve for the Falkner loading coefficients $a_{m,n}$ for the entire surface so the spanwise and chordwise integration could be performed. This procedure for evaluating the induced-camber correction is identical to that used in reference 4. The induced-camber corrections are also applied to the lift parameters computed by the Falkner method.

From figure 11 or 12,

$$\begin{aligned} \left(\Delta c_{h\alpha} \right)_{SC} &= -0.0008 \\ \left(c_{h\alpha} \right)_{LS} &= (-0.0057)(0.707)(0.6949) + (-0.0008) \\ &= -0.0036 \end{aligned}$$

The equation on page 12, reference 4, now is

$$\begin{aligned} \left(c_{h\delta} \right)_{LS} &= \left(c_{h\delta} \right)_{\Lambda=0} \cos \Lambda \cos \Lambda_h + \\ &\quad \left[\left(\alpha_{\delta} \right)_{c_L} \right]_{\Lambda=0} (\cos \Lambda_h) \left[\left(c_{h\alpha_0} \right)_{\Lambda=0} (\cos \Lambda) - \left(c_{h\alpha} \right)_{LS} \right] \\ &= (-0.0114)(0.707)(0.756) + (-0.60)(0.756) \left[-0.0040 - \right. \\ &\quad \left. (-0.0036) \right] \\ &= -0.0059 \end{aligned}$$

Method 2

For this method the factor $\left(1 - \frac{\alpha_1}{\alpha}\right)$ is computed from the lift-curve slopes presented in reference 9. The induced-camber correction to $C_{h\alpha}$, $\left(\Delta C_{h\alpha}\right)_{SC}$ is computed in the same manner as that of method 1 or reference 4.

From reference 9, $C_{L\alpha} = 0.055$ for the model having an aspect ratio of 4.5 and swept back 45° . Correcting the section lift-curve slope for sweep,

$$\begin{aligned}\left(c_{l\alpha_0}\right)_\Lambda &= \left(c_{l\alpha_0}\right)_{\Lambda=0} \cos \Lambda \\ &= (0.108)(0.707) = 0.0764\end{aligned}$$

Compute α_1/C_L from

$$\begin{aligned}\frac{\alpha_1}{C_L} &= \frac{1}{C_{L\alpha}} - \frac{1}{\left(c_{l\alpha_0}\right)_\Lambda} \\ &= \frac{1}{0.055} - \frac{1}{0.0764} = 5.08^\circ\end{aligned}$$

The angle of attack per unit lift coefficient is

$$\frac{\alpha}{C_L} = \frac{1}{C_{L\alpha}} = \frac{1}{0.055} = 18.18^\circ$$

Then

$$\frac{\alpha_1}{\alpha} = \frac{5.08^\circ}{18.18^\circ} = 0.279$$

and

$$\left(1 - \frac{\alpha_1}{\alpha}\right) = 0.721$$

The parameter $C_{L\delta}$ is $\left(c_{l\delta}\right)_{\Lambda=0} \cos \Lambda \cos \Lambda_h \left(1 - \frac{\alpha_1}{\alpha}\right)$

or

$$\begin{aligned} C_{L\delta} &= \left[\left(\alpha_{\delta} \right)_{c_l} \right]_{\Lambda=0} \cos \Lambda_h C_{L\alpha} \\ &= (0.60)(0.756)(0.055) \\ &= 0.025 \end{aligned}$$

The flap-effectiveness parameter is

$$\left(\alpha_{\delta} \right)_{c_L} = - \frac{C_{L\delta}}{C_{L\alpha}} = - \frac{0.025}{0.055} = -0.455$$

and

$$\left(C_{h\alpha} \right)_{LS} = \left(C_{h\alpha_0} \right)_{\Lambda=0} \cos \Lambda \left(1 - \frac{\alpha_1}{\alpha} \right) + \left(\Delta C_{h\alpha} \right)_{SC}$$

From figure 11 or 12,

$$\left(\Delta C_{h\alpha} \right)_{SC} = -0.0008$$

$$\begin{aligned} \left(C_{h\alpha} \right)_{LS} &= (-0.0057)(0.707)(0.721) + (-0.0008) \\ &= -0.0037 \end{aligned}$$

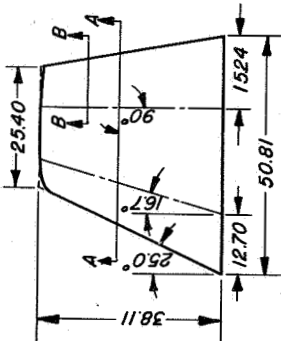
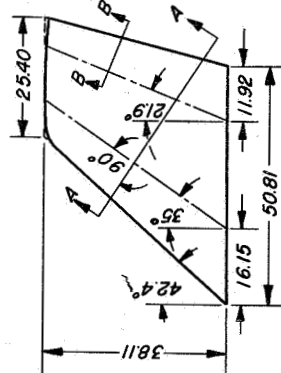
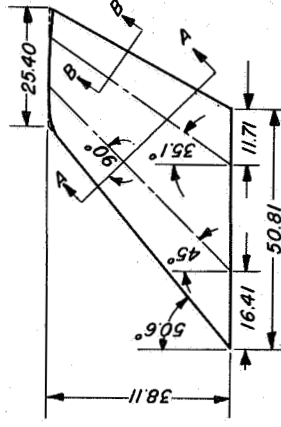
$$\begin{aligned} \left(C_{h\delta} \right)_{LS} &= \left(C_{h\delta} \right)_{\Lambda=0} \cos \Lambda \cos \Lambda_h + \left(\alpha_{\delta} \right)_{c_L} \left[\left(C_{h\alpha_0} \right)_{\Lambda=0} \cos \Lambda - \left(C_{h\alpha} \right)_{LS} \right] \\ &= (-0.0114)(0.707)(0.756) + (-0.455) \left[(-0.0040) - (-0.0037) \right] \\ &= -0.0060 \end{aligned}$$

REFERENCES

1. Swanson, Robert S., and Gillis, Clarence L.: Limitations of Lifting-Line Theory for Estimation of Aileron Hinge-Moment Characteristics. NACA CB '3L02, 1943.
2. Swanson, Robert S., and Crandall, Stewart M.: Lifting-Surface-Theory Aspect-Ratio Corrections to the Lift and Hinge-Moment Parameters for Full-Span Elevators on Horizontal Tail Surfaces. NACA Rep. 911, 1948.
3. Swanson, Robert S., Crandall, Stewart M., and Miller, Sadie: A Lifting-Surface-Theory Solution and Tests of an Elliptic Tail Surface of Aspect Ratio 3 with a 0.5-Chord 0.85-Span Elevator. NACA TN 1275, 1947.
4. Jones, Arthur L., and Sluder, Loma: An Application of Falkner's Surface-Loading Method to Predictions of Hinge-Moment Parameters for Swept-Back Wings. NACA TN 1506, 1948.
5. Falkner, V. M.: The Calculation of Aerodynamic Loading on Surfaces of Any Shape. R. & M. No. 1910, British A. R. C., 1943.
6. Van Dorn, Nicholas H., and DeYoung, John: A Comparison of Three Theoretical Methods of Calculating Span Load Distribution on Swept Wings. NACA TN 1476, 1947.
7. Dods, Jules B., Jr: Wind-Tunnel Investigation of Horizontal Tails.
 - I - Unswept and 35° Swept-Back Plan Forms of Aspect Ratio 3. NACA RM A7K24, 1948.
 - II - Unswept and 35° Swept-Back Plan Forms of Aspect Ratio 4.5. NACA RM A8B11, 1948.
 - III - Unswept and 35° Swept-Back Plan Forms of Aspect Ratio 6. NACA RM A8H30, 1948.
 - IV - Unswept Plan Form of Aspect Ratio 2 and a Two-Dimensional Model. NACA RM A8J21, 1948.
 - V - 45° Swept-Back Plan Form of Aspect Ratio 2. NACA RM A9D05, 1949.
8. Crane, Robert M.: Computation of Hinge-Moment Characteristics of Horizontal Tails from Section Data. NACA CB 5B05, 1945.
9. DeYoung, John, and Harper, Charles W.: Theoretical Symmetric Span Loading at Subsonic Speeds for Wings Having Arbitrary Plan Form. NACA Rep. 921, 1948.

10. Toll, Thomas A., and Schneider, Leslie E.: Approximate Relations for Hinge-Moment Parameters of Control Surfaces on Swept Wings at Low Mach Numbers. NACA TN 1711, 1948.

TABLE I.-GEOMETRY OF THE MODELS
 [NACA 64A010 airfoil section; area of 10.08 ft²; taper ratio, 0.5]

Aspect ratio 2		
$\Lambda, 16.7^\circ$	$\Lambda, 35^\circ$ [Theoretical calculations only]	$\Lambda, 45^\circ$
Flap area, 3.025 ft ² \bar{c} , 3.293 ft $2M_A$, 2.987 ft ³	Flap area, 2.366 ft ² \bar{c} , 3.293 ft $2M_A$, 1.696 ft ³	Flap area, 2.324 ft ² \bar{c} , 3.293 ft $2M_A$, 1.444 ft ³
		

All dimensions in inches.

The NACA 64A010 airfoil section is parallel to section A-A.

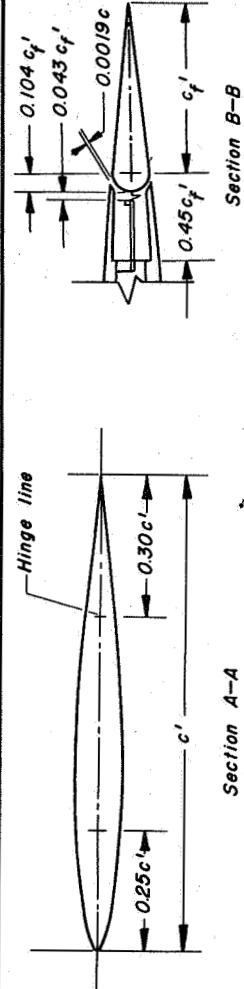
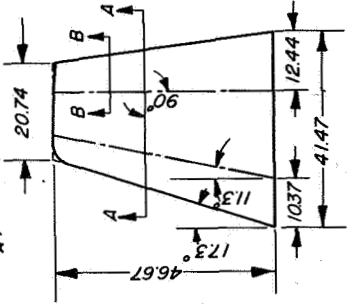
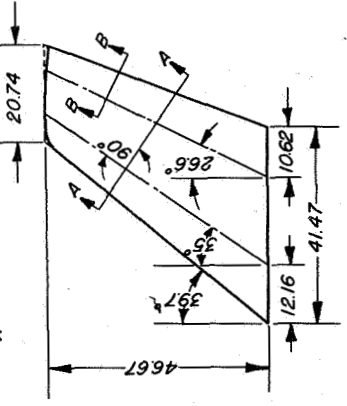
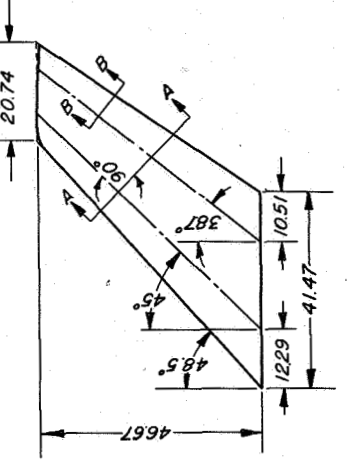
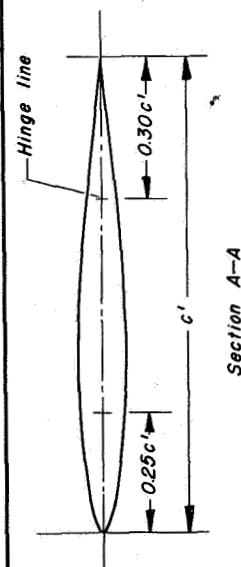
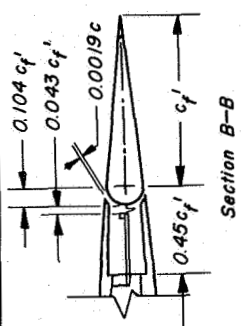


TABLE I.-CONTINUED.

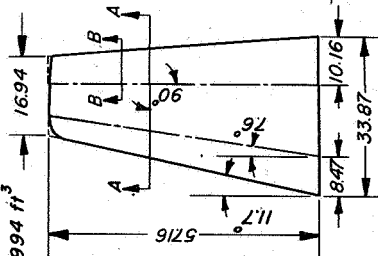
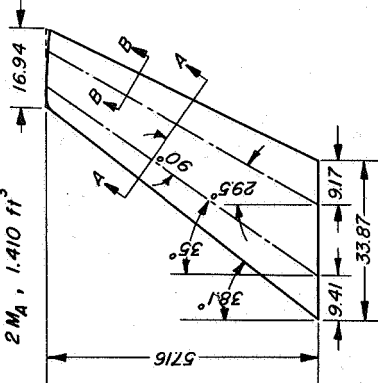
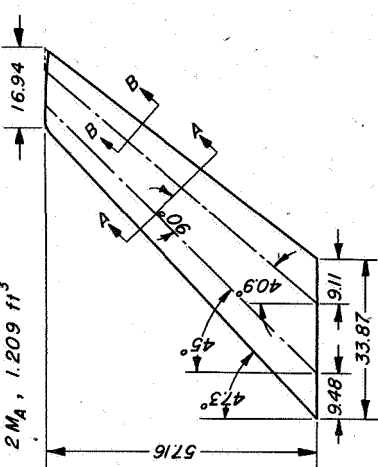
Aspect ratio 3		
$\Lambda, 11.3^\circ$	$\Lambda, 35^\circ$	$\Lambda, 45^\circ$
<p>Flap area, 3.025 ft² \bar{c}, 2.688 ft $2M_A$, 2.439 ft³</p> 	<p>Flap area, 2.581 ft² \bar{c}, 2.688 ft $2M_A$, 1.565 ft³</p> 	<p>Flap area, 2.553 ft² \bar{c}, 2.688 ft $2M_A$, 1.357 ft³</p> 



All dimensions in inches.

The NACA 64A10 airfoil section is parallel to section A-A.

TABLE I.-CONTINUED.

Aspect ratio 4.5		
$\Lambda, 7.6^\circ$	$\Lambda, 35^\circ$	$\Lambda, 45^\circ$ [Theoretical calculations only]
Flap area, 3.025 ft ² \bar{c} , 2.195 ft $2M_A$, 1.994 ft ³	Flap area, 2.729 ft ² \bar{c} , 2.195 ft $2M_A$, 1.410 ft ³	Flap area, 2.712 ft ² \bar{c} , 2.195 ft $2M_A$, 1.209 ft ³
		

All dimensions in inches.

The NACA 64A010 airfoil section is parallel to section A-A.

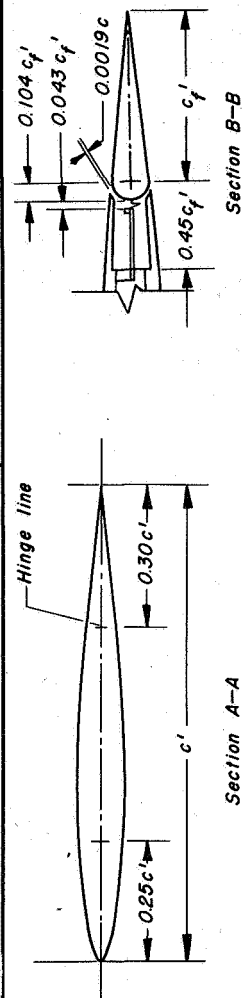
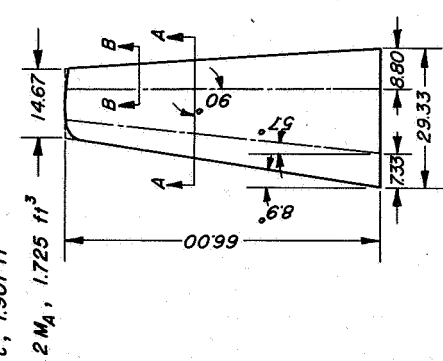
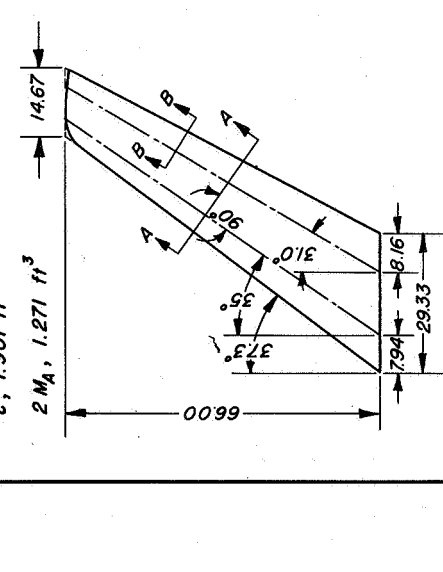
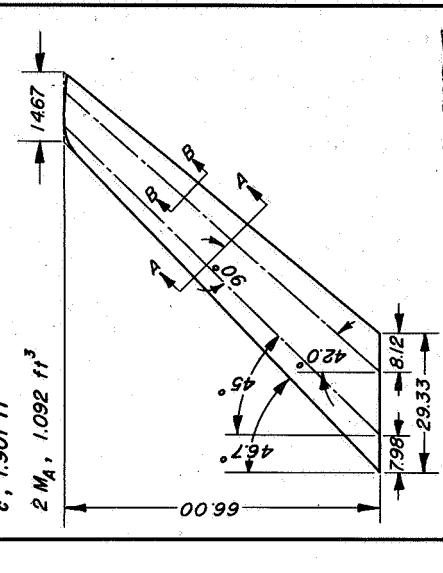


TABLE I.-CONCLUDED.

Aspect ratio 6		
$\Delta, 5.7^\circ$	$\Delta, 35^\circ$	$\Delta, 45^\circ$ [Theoretical calculations only]
<p>Flap area, 3.025 ft² \bar{c}, 1.901 ft $2M_A$, 1.725 ft³</p> 	<p>Flap area, 2.803 ft² \bar{c}, 1.901 ft $2M_A$, 1.271 ft³</p> 	<p>Flap area, 2.791 ft² \bar{c}, 1.901 ft $2M_A$, 1.092 ft³</p> 

All dimensions in inches.

The NACA 64A010 airfoil section is parallel to section A-A.

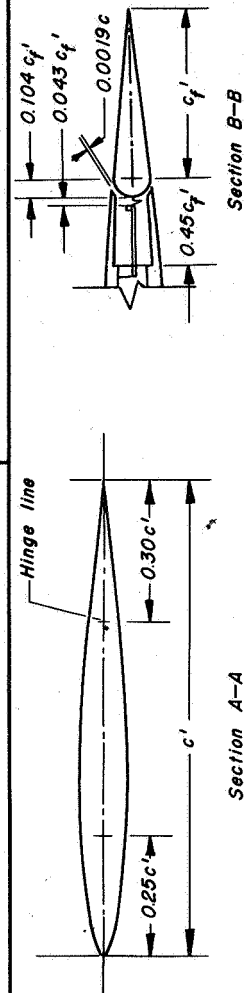


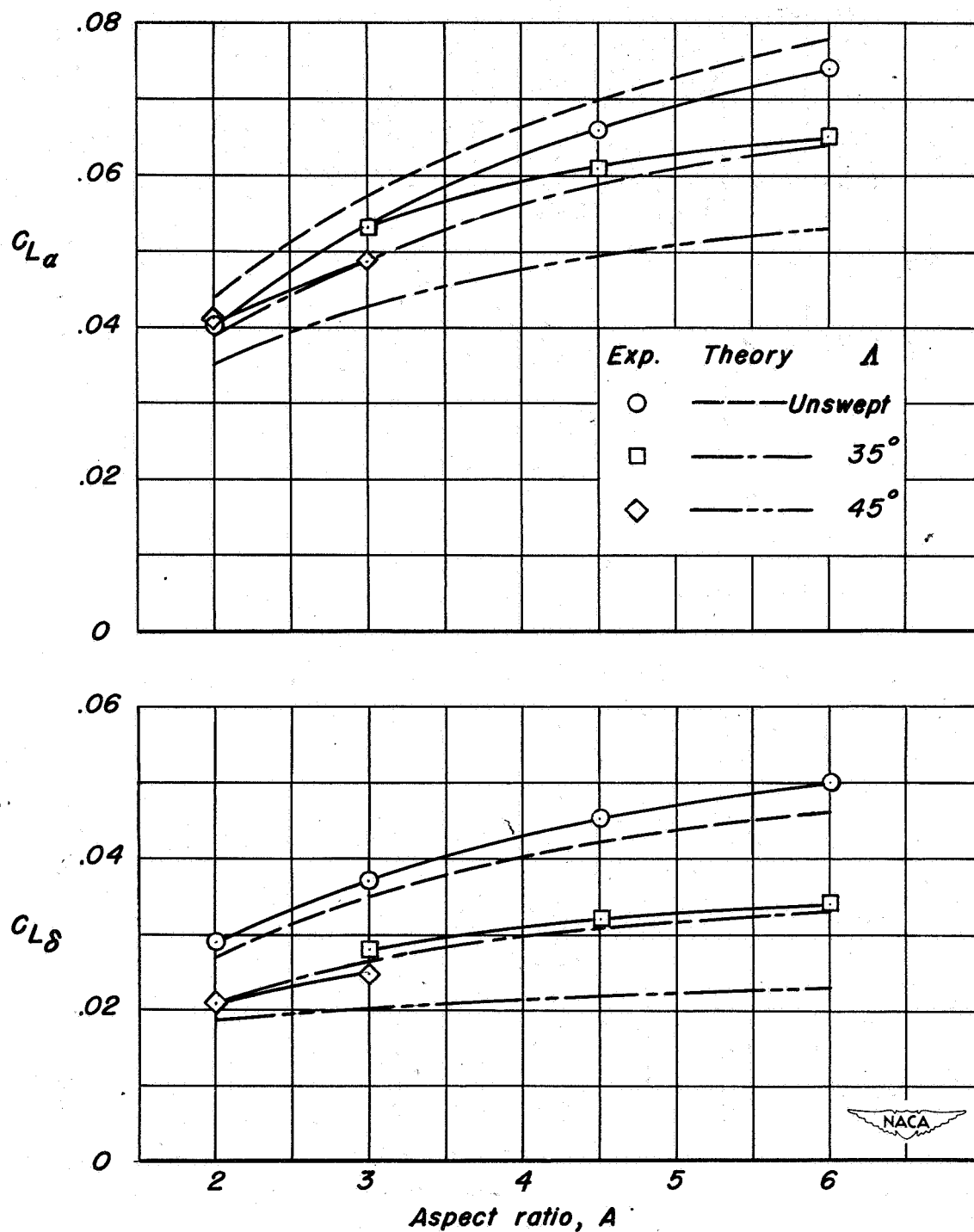
TABLE II.- SUMMARY OF THE EXPERIMENTAL AND THEORETICAL LIFT AND HINGE-MOMENT PARAMETERS

[NACA 64A010 airfoil section; flap-chord ratio, 0.30; taper ratio, $\lambda = 0.50$]

Model		Lift and hinge-moment ^a parameters ^b																							
Aspect ratio, A	Angle of sweep- back, Λ , (deg)	$C_{L\alpha}$						$C_{L\delta}$						$C_{h\alpha}$						$C_{h\delta}$					
		Method						Method						Method						Method					
		Exp	1	2	3	4	5°	Exp	1	2	3	4	5°	Exp	1	2	3	4	5°	Exp	1	2	3	4	5°
2	16.7	0.040	0.044	0.043	0.043	0.053	0.044	0.029	0.027	0.024	0.024	0.030	0.029	-0.0002	-0.0006	-0.0001	-0.0001	-0.0008	-0.0006	-0.0071	-0.0080	-0.0079	-0.0079	-0.0067	-0.0073
2	35 ^d	---	.039	.042	.042	.049	---	---	.021	.023	.023	.027	---	---	---	---	---	---	---	---	---	---	---	---	---
2	45	.041	.035	.040	.040	.045	---	.021	.019	.020	.020	.022	---	---	---	---	---	---	---	---	---	---	---	---	---
3	11.3	.053	.057	.055	.055	.064	.056	.037	.035	.033	.033	.038	.036	---	---	---	---	---	---	---	---	---	---	---	---
3	35	.053	.049	.052	.052	.057	---	.028	.027	.028	.028	.031	---	---	---	---	---	---	---	---	---	---	---	---	---
3	45	.049	.043	.048	.048	.052	---	.025	.020	.023	.023	.024	---	---	---	---	---	---	---	---	---	---	---	---	---
4.5	7.6	.066	.070	.067	.067	.074	.071	.045	.042	.040	.040	.044	.044	---	---	---	---	---	---	---	---	---	---	---	---
4.5	35	.061	.059	.060	.060	.065	---	.032	.031	.031	.031	.034	---	---	---	---	---	---	---	---	---	---	---	---	---
4.5	45 ^d	---	.049	.055	.055	.058	---	---	.022	.025	.025	.026	---	---	---	---	---	---	---	---	---	---	---	---	---
6	5.7	.074	.078	.075	.075	.081	.076	.050	.046	.045	.045	.048	.047	---	---	---	---	---	---	---	---	---	---	---	---
6	35	.065	.064	.065	.065	.070	---	.034	.033	.033	.033	.036	---	---	---	---	---	---	---	---	---	---	---	---	---
6	45 ^d	---	.053	.058	.058	.062	---	---	.023	.026	.026	.028	---	---	---	---	---	---	---	---	---	---	---	---	---

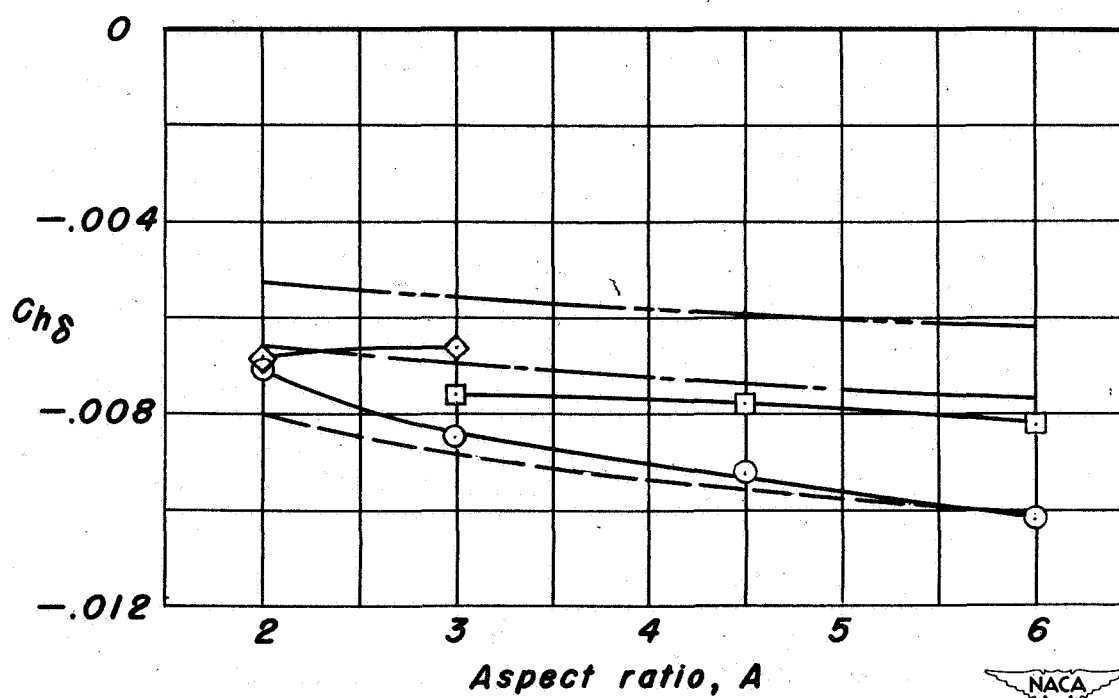
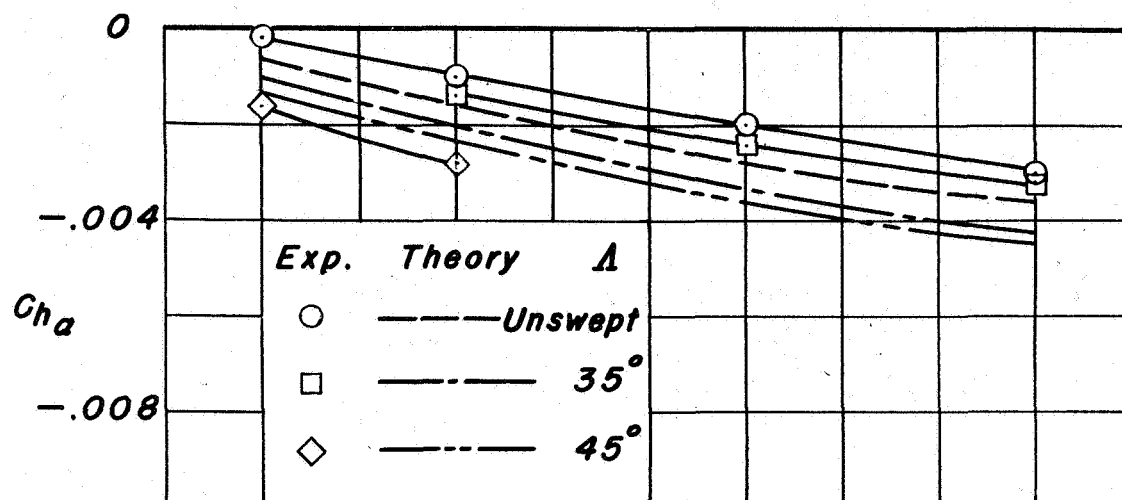
^aHinge-moment coefficients based on $2M_A$.^bExperimentally, $C_{L\alpha} = 0.108$; $C_{L\delta} = 0.065$; $C_{h\alpha} = -0.0057$; $C_{h\delta} = -0.0114$.^cMethod 5 is not applicable to swept-back airfoils.^dTheoretical calculations only.

NACA



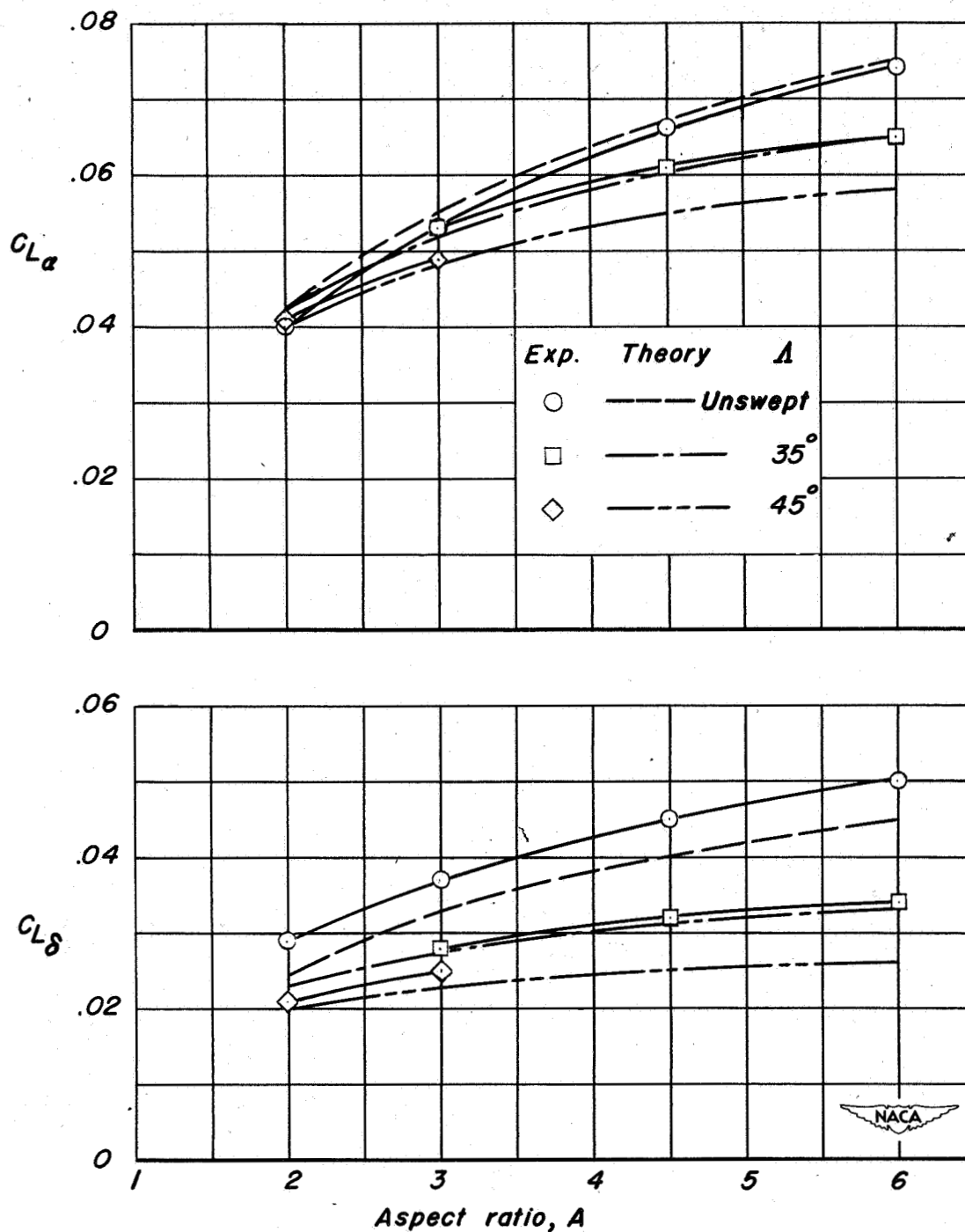
(a) Lift parameters.

Figure 1.—Comparison of the experimental lift and hinge-moment parameters as a function of the aspect ratio with those calculated by Method 1.



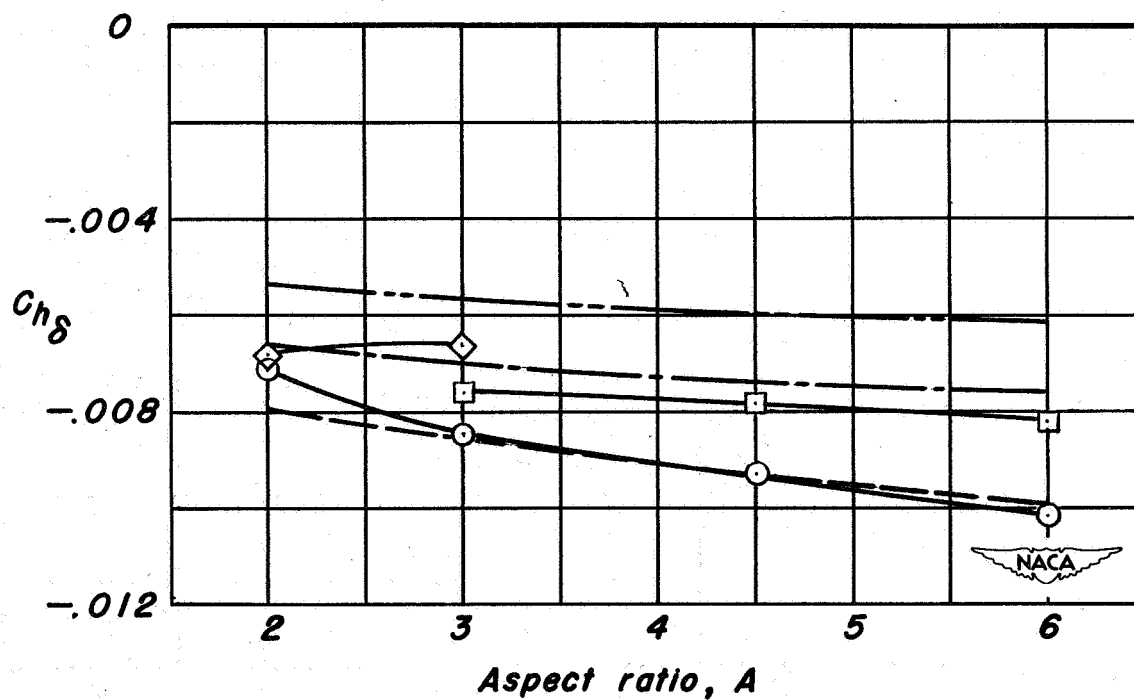
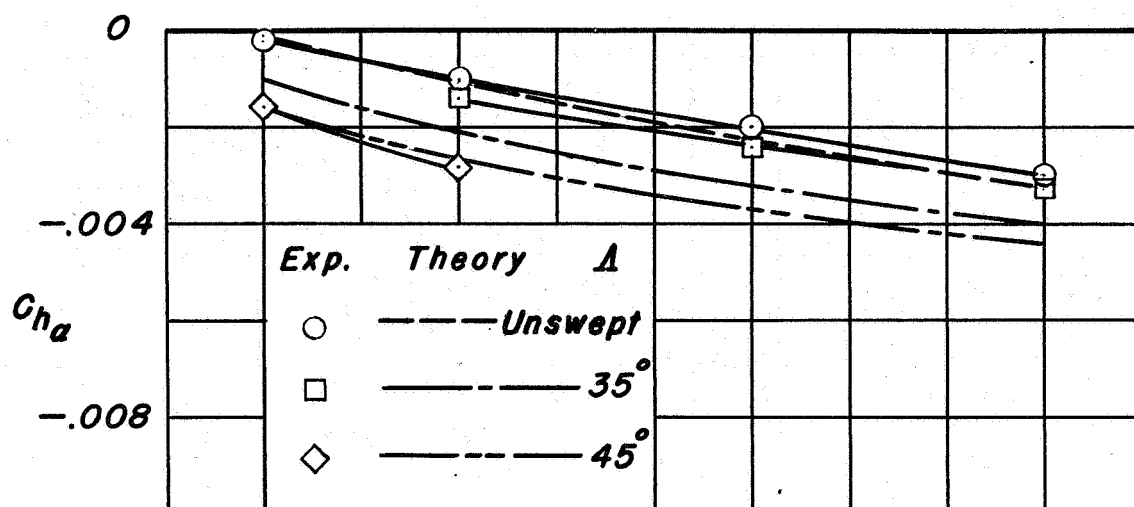
(b) Hinge-moment parameters.

Figure 1.—Concluded.



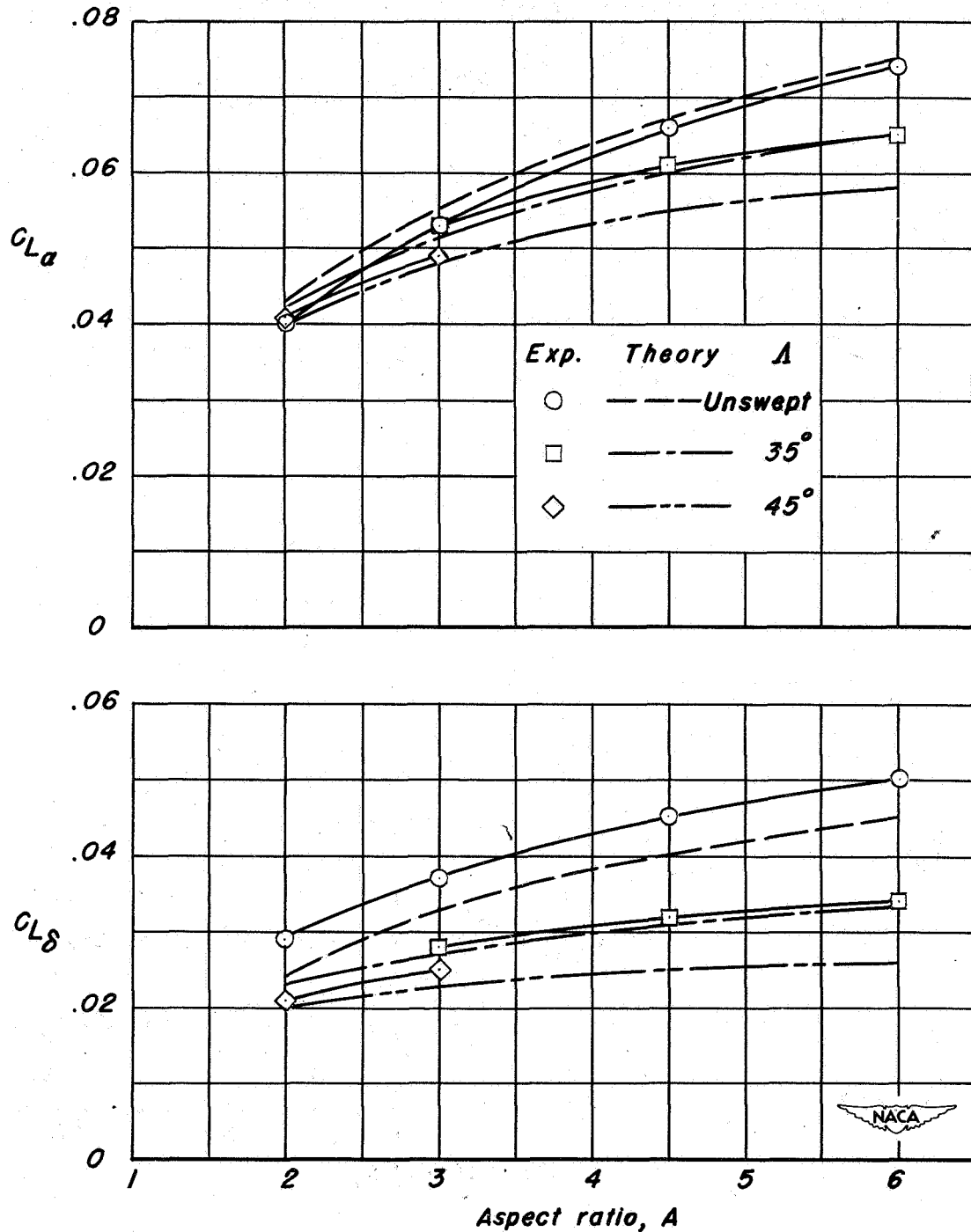
(a) Lift parameters.

Figure 2.—Comparison of the experimental lift and hinge-moment parameters as a function of the aspect ratio with those calculated by Method 2.



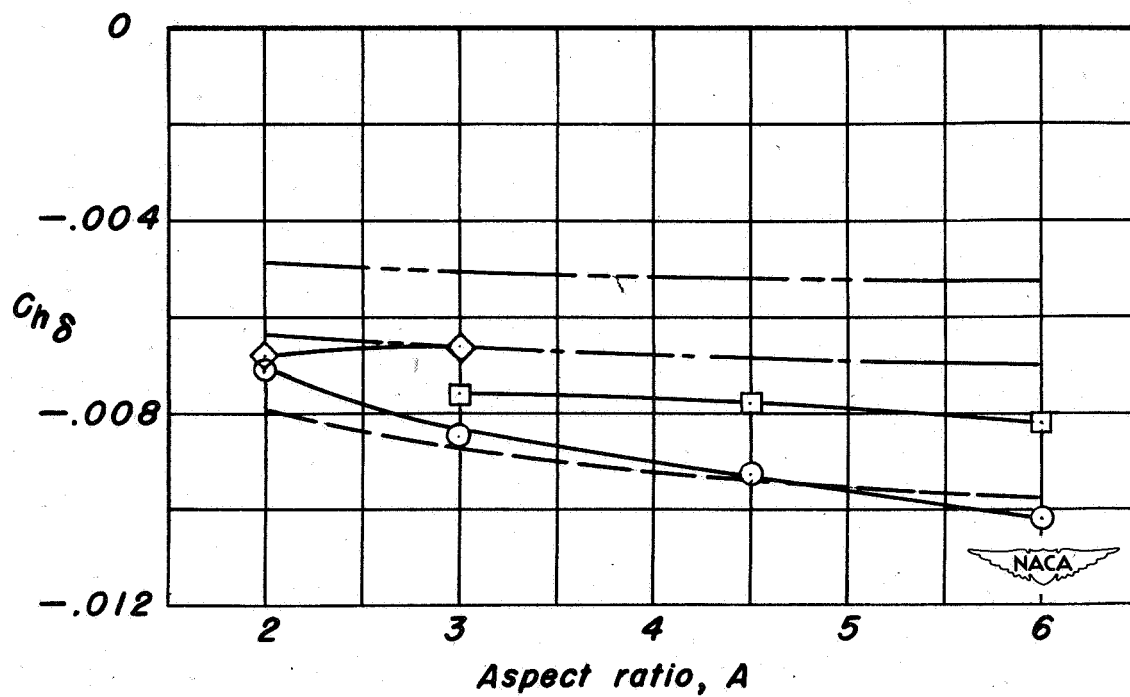
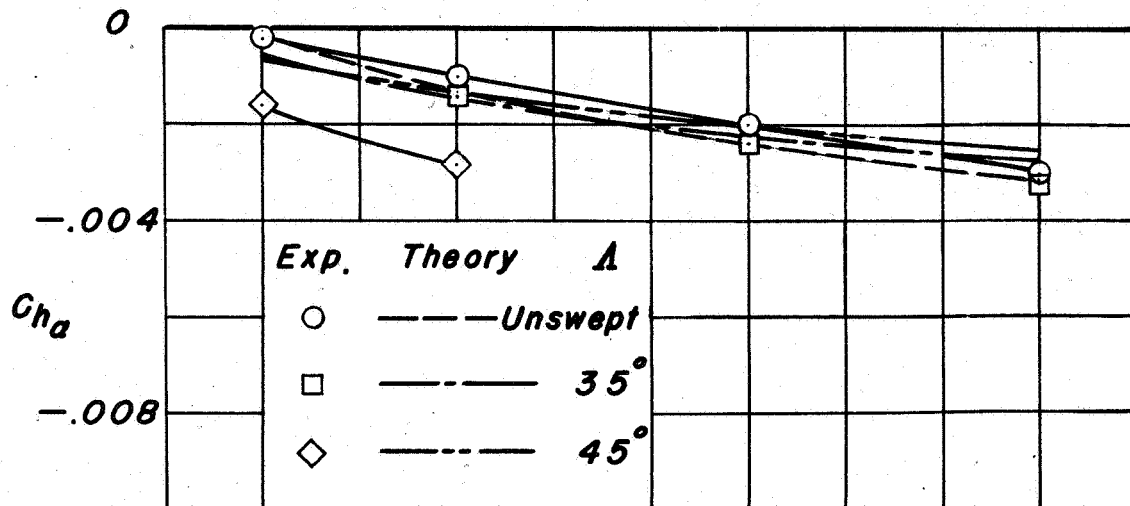
(b) Hinge-moment parameters.

Figure 2.—Concluded.



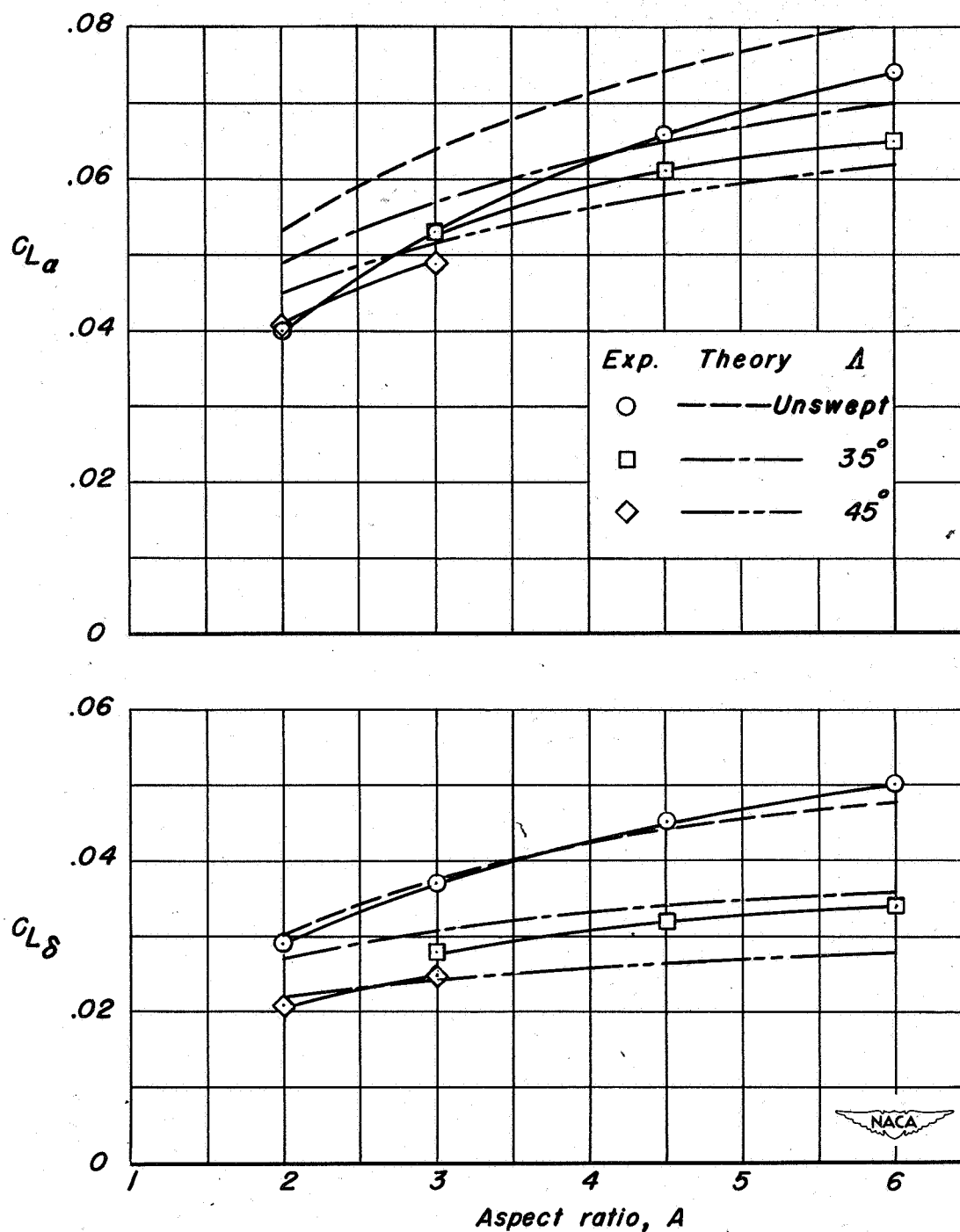
(a) Lift parameters.

Figure 3.—Comparison of the experimental lift and hinge-moment parameters as a function of the aspect ratio with those calculated by Method 3.



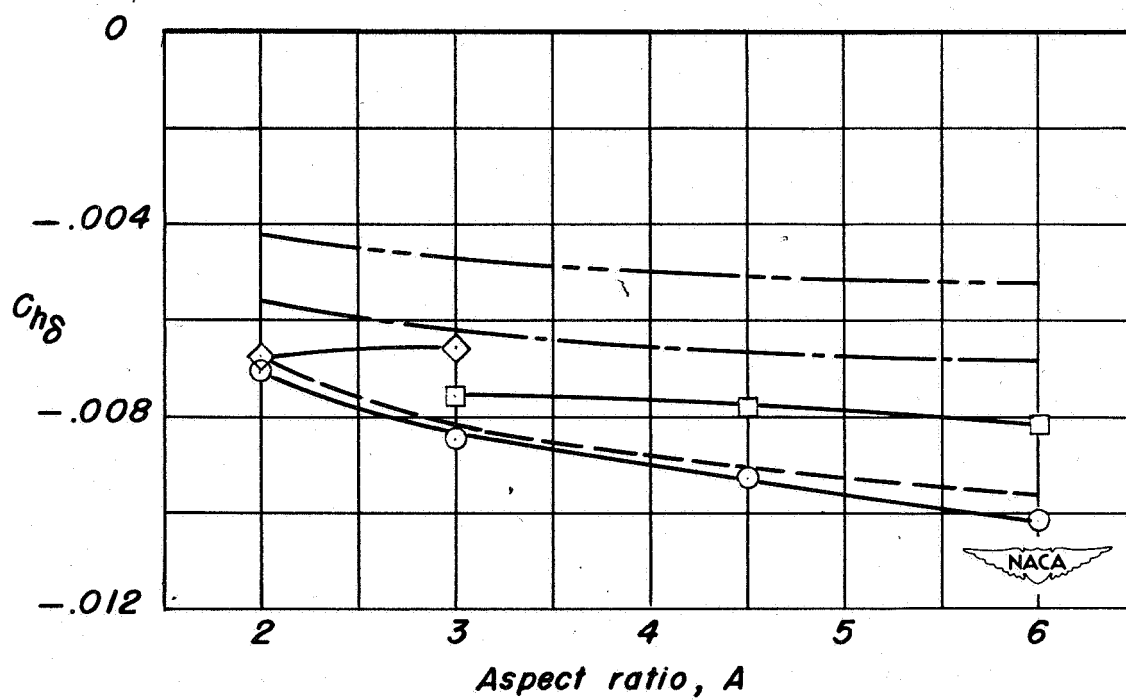
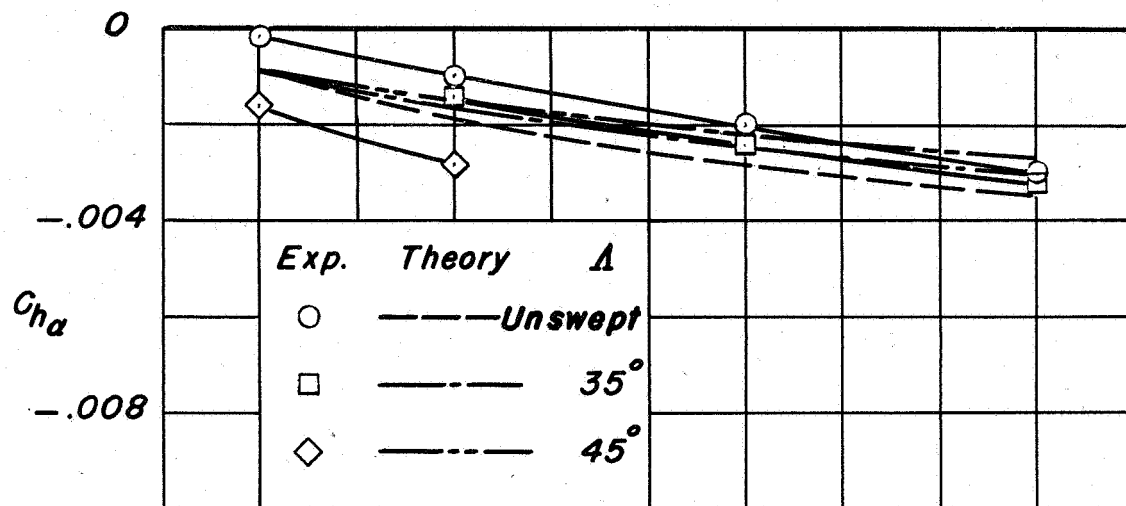
(b) Hinge-moment parameters.

Figure 3.—Concluded.



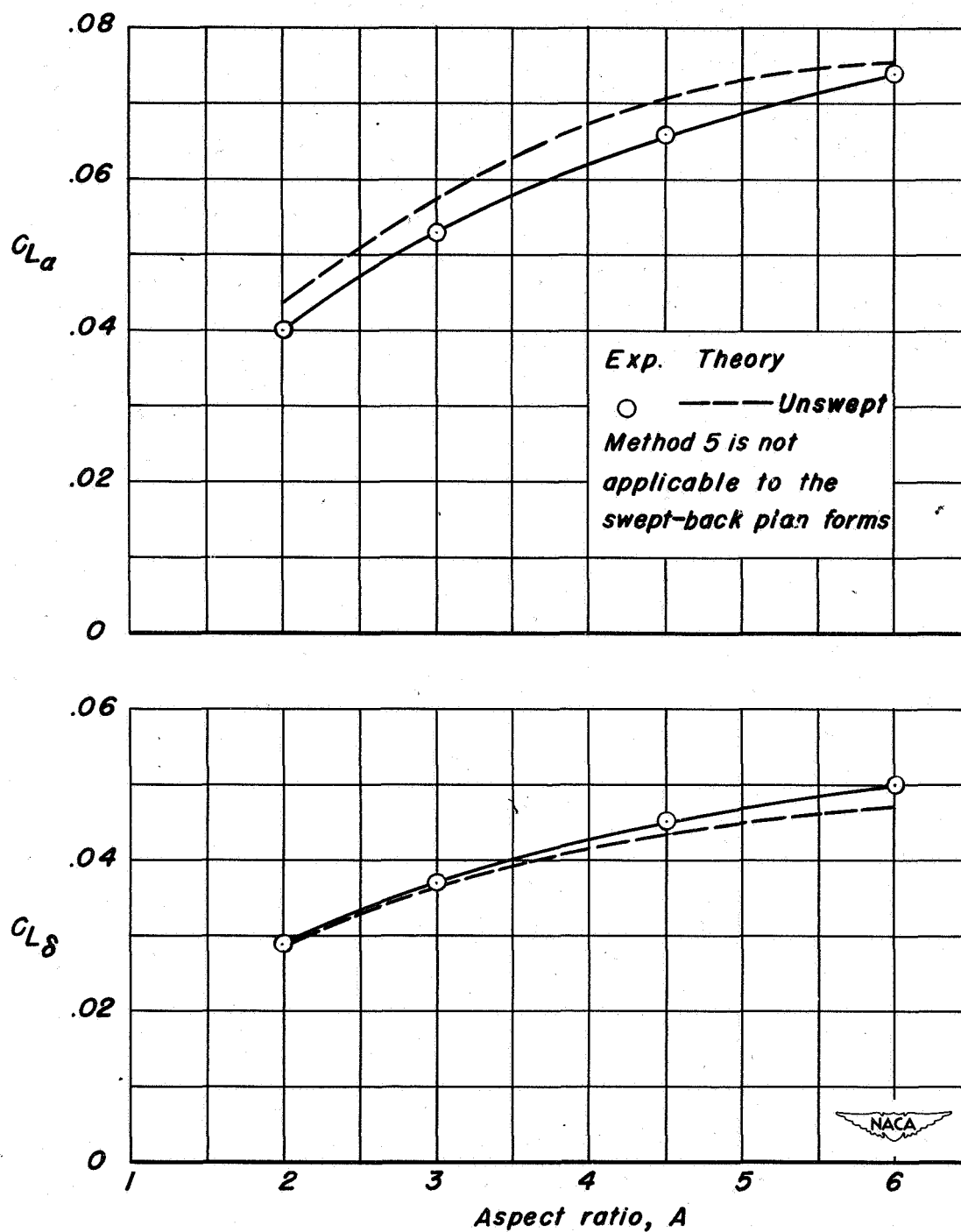
(a) Lift parameters.

Figure 4.— Comparison of the experimental lift and hinge-moment parameters as a function of the aspect ratio with those calculated by Method 4.



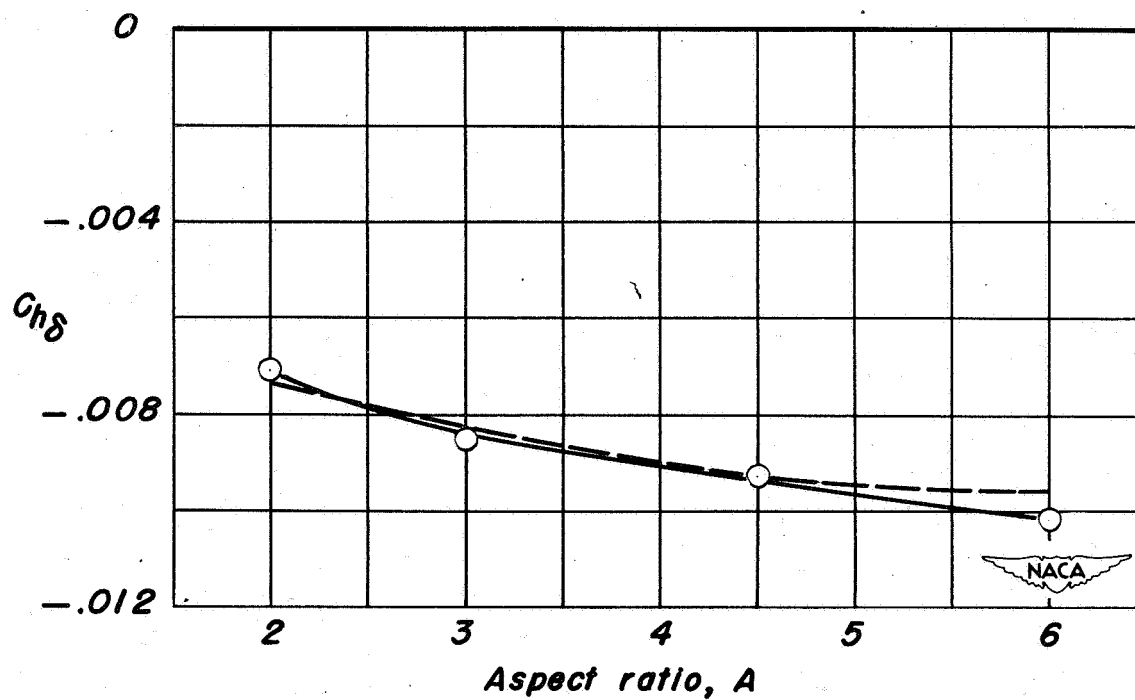
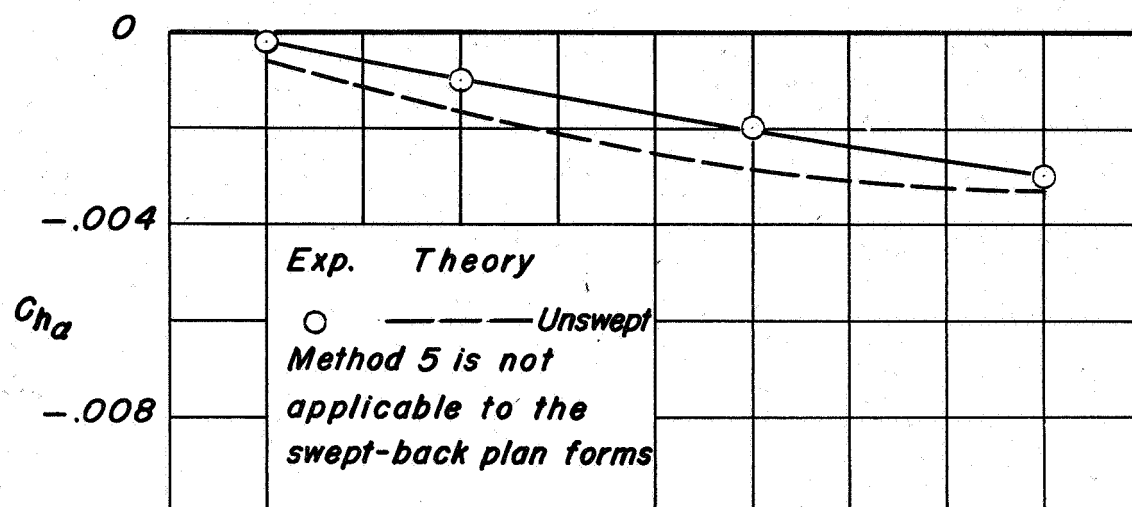
(b) Hinge-moment parameters.

Figure 4.—Concluded.



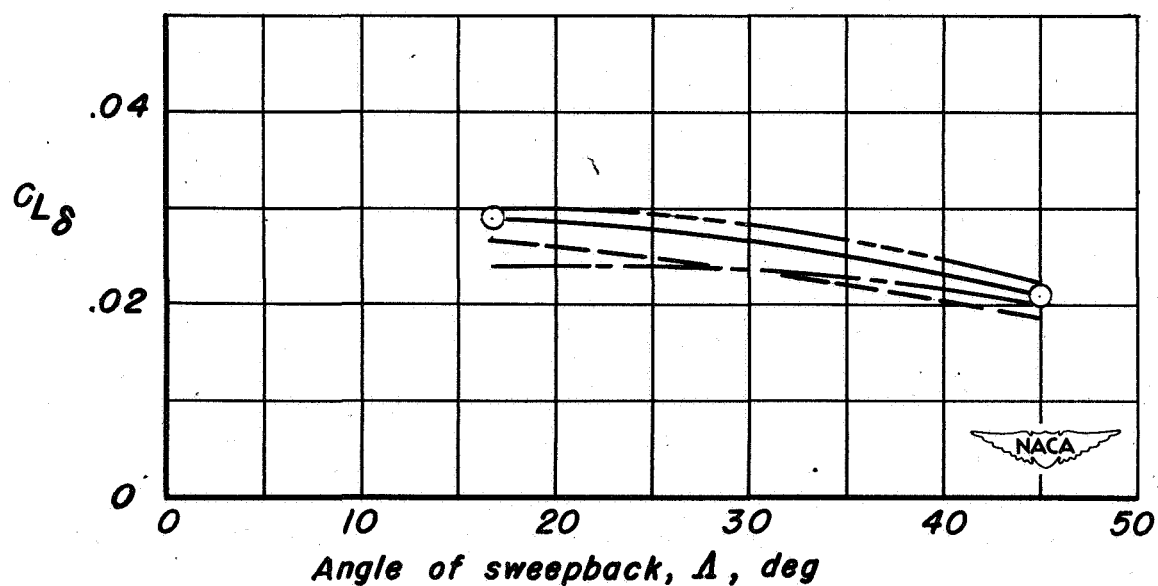
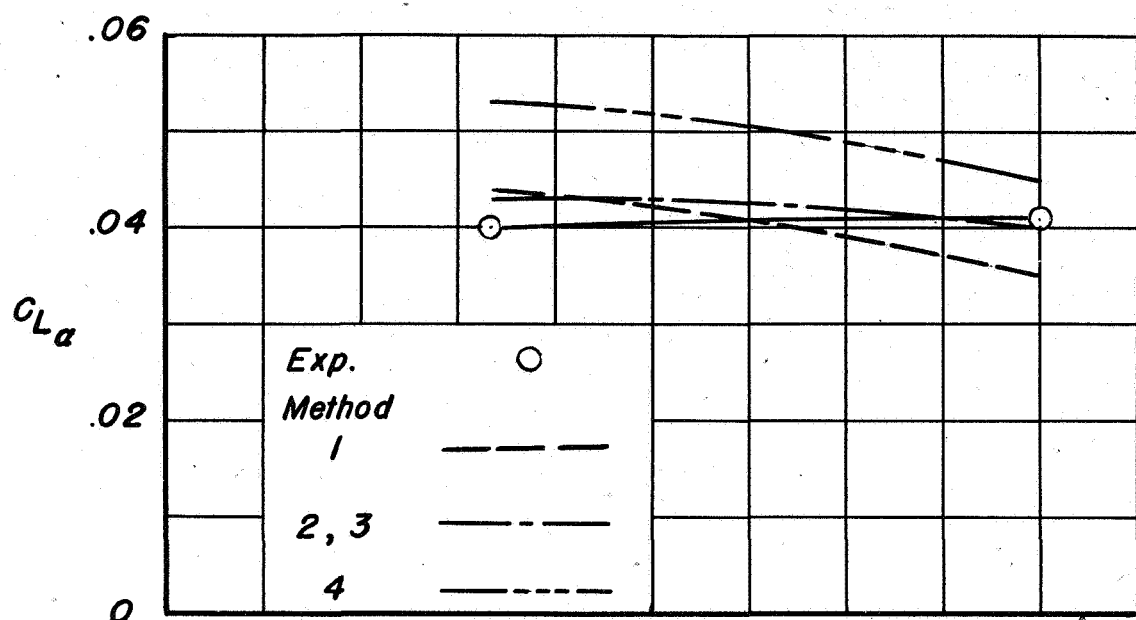
(a) Lift parameters.

Figure 5.—Comparison of the experimental lift and hinge-moment parameters as a function of the aspect ratio with those calculated by Method 5.



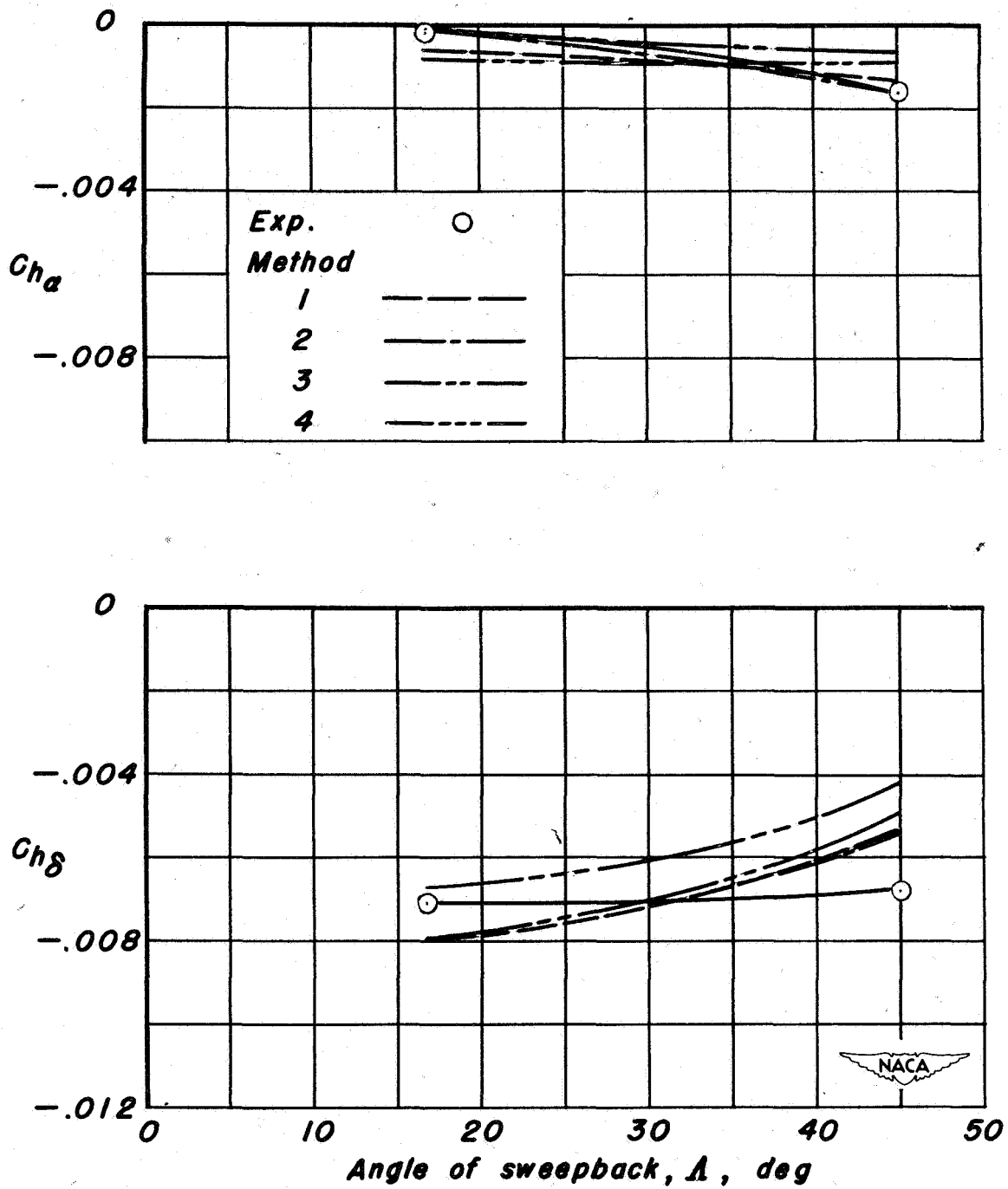
(b) Hinge-moment parameters.

Figure 5.—Concluded.



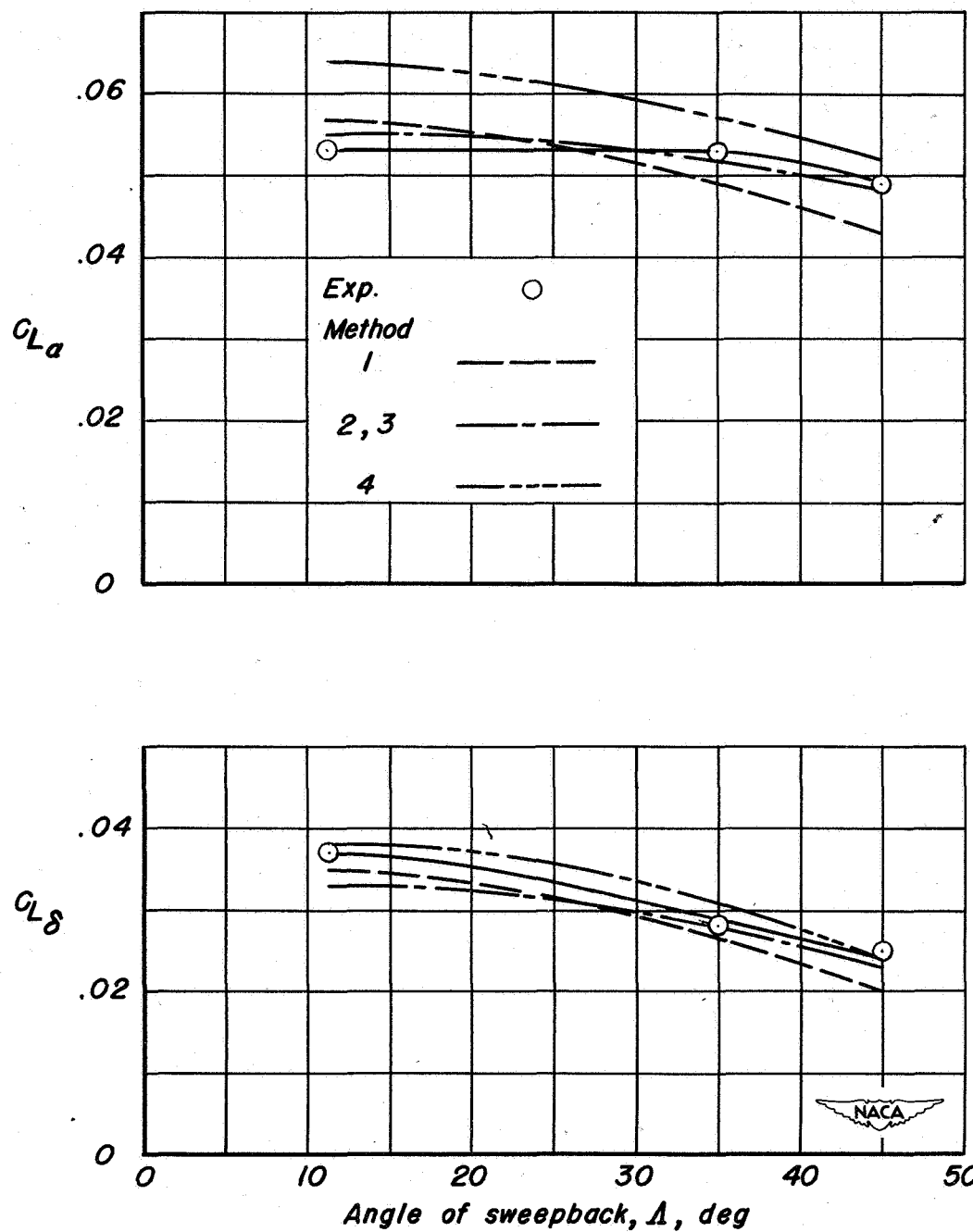
(a) Lift parameters.

Figure 6.—Comparison of the experimental and calculated lift and hinge-moment parameters as a function of the angle of sweepback. Aspect ratio 2.



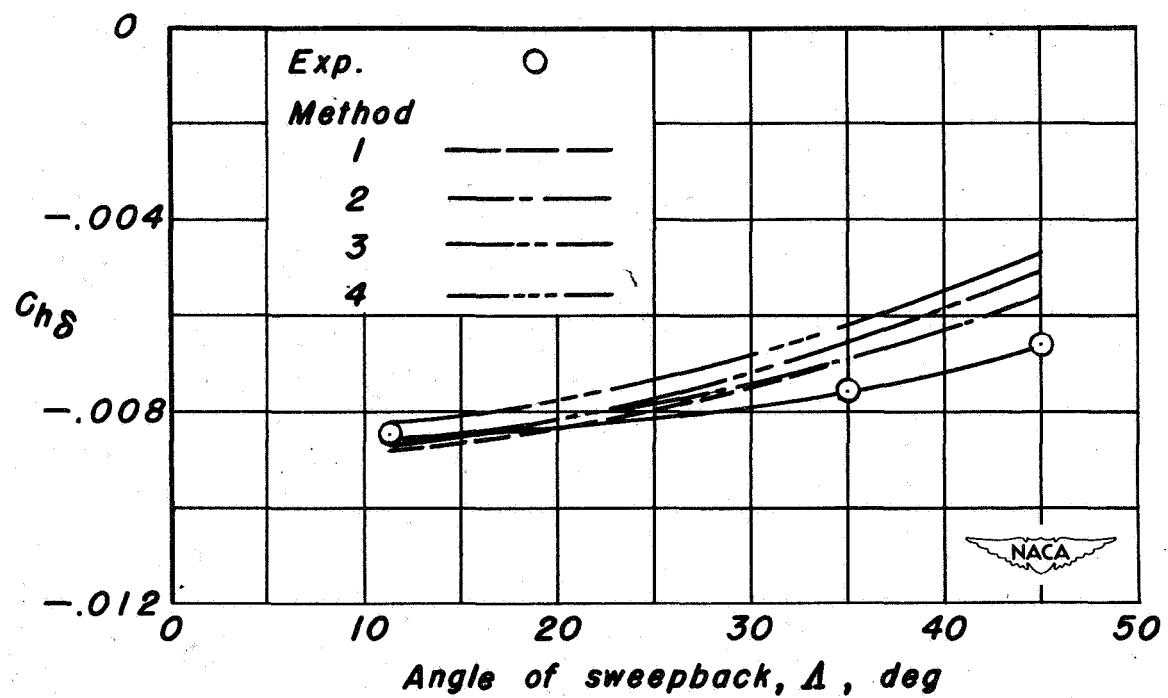
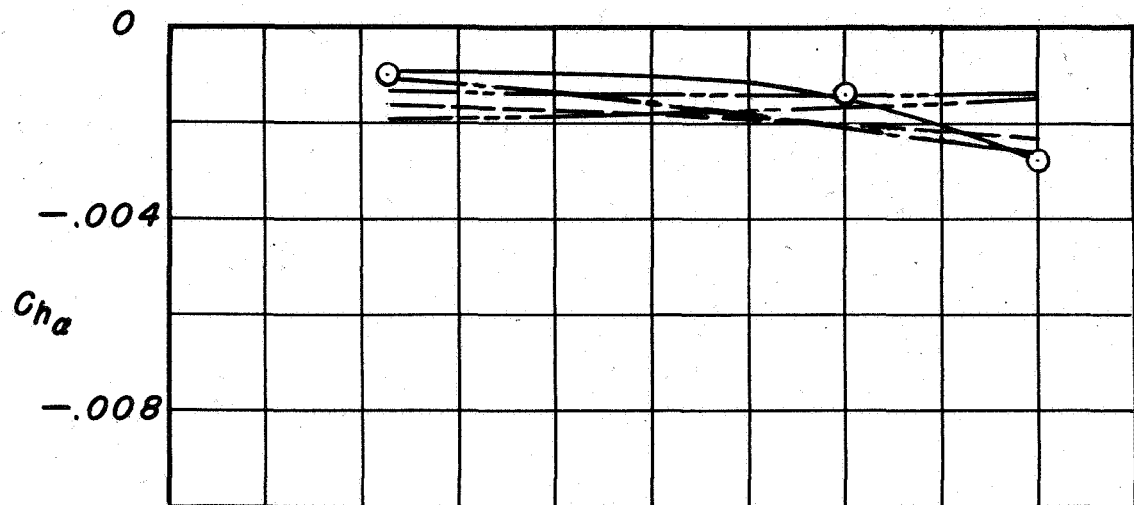
(b) Hinge-moment parameters.

Figure 6.—Concluded.



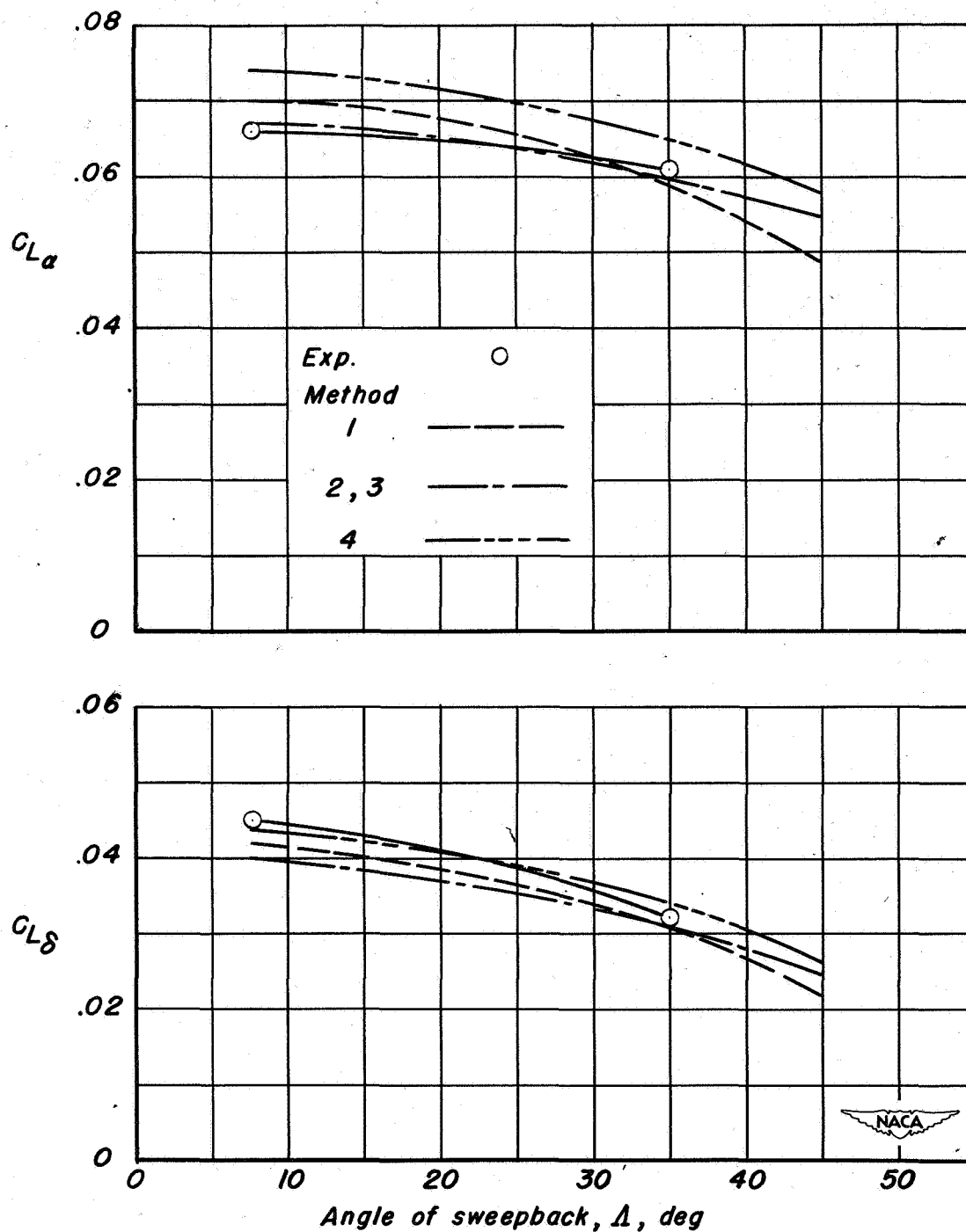
(a) Lift parameters.

Figure 7.—Comparison of the experimental and calculated lift and hinge-moment parameters as a function of the angle of sweepback. Aspect ratio 3.



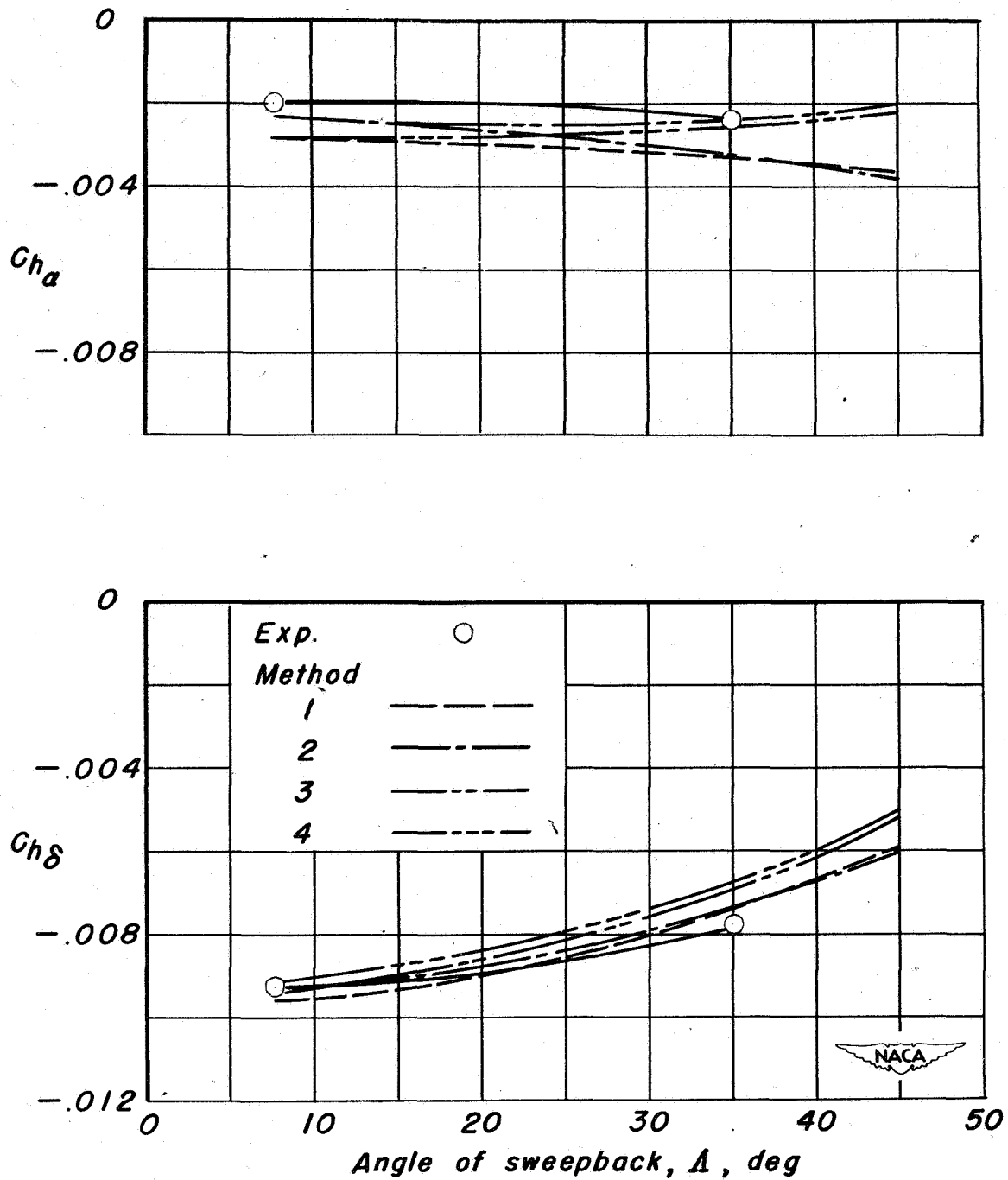
(b) Hinge-moment parameters.

Figure 7.—Concluded.



(a) Lift parameters.

Figure 8.—Comparison of the experimental and calculated lift and hinge-moment parameters as a function of the angle of sweepback. Aspect ratio 4.5.



(b) Hinge-moment parameters.

Figure 8.—Concluded.

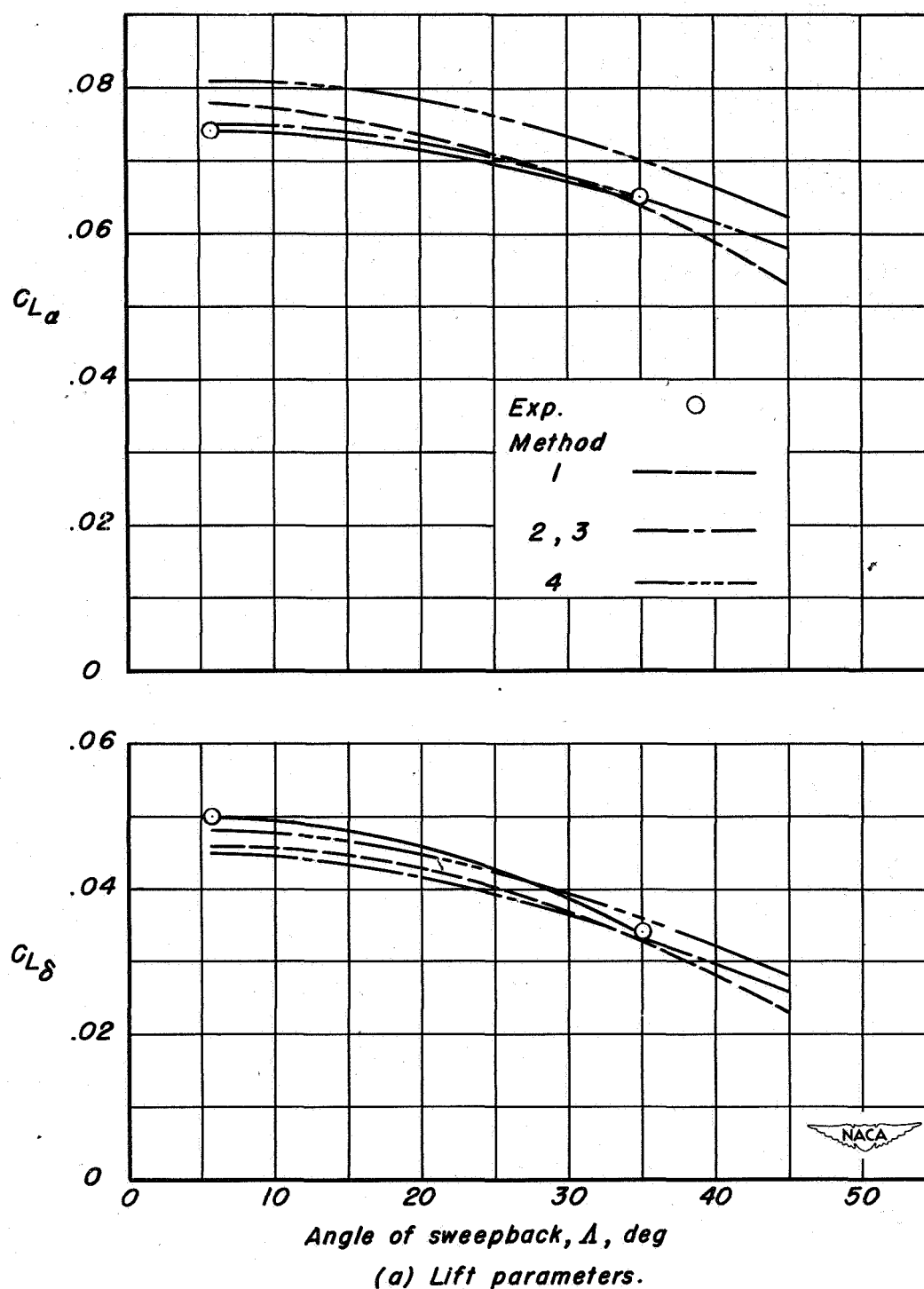
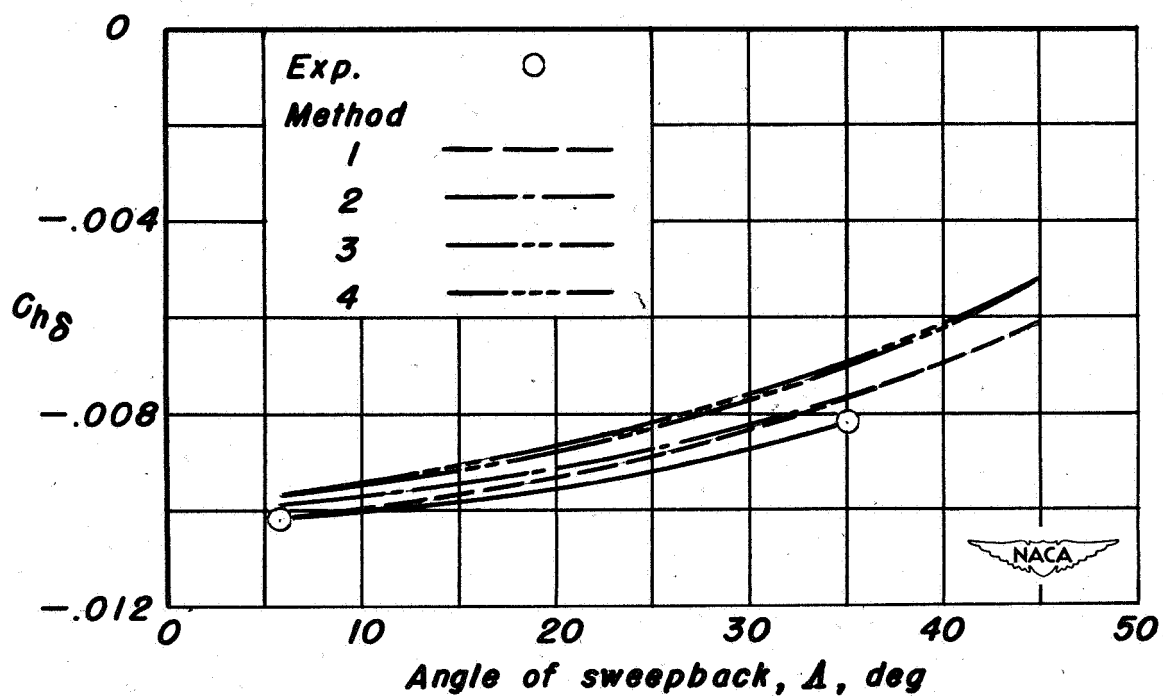
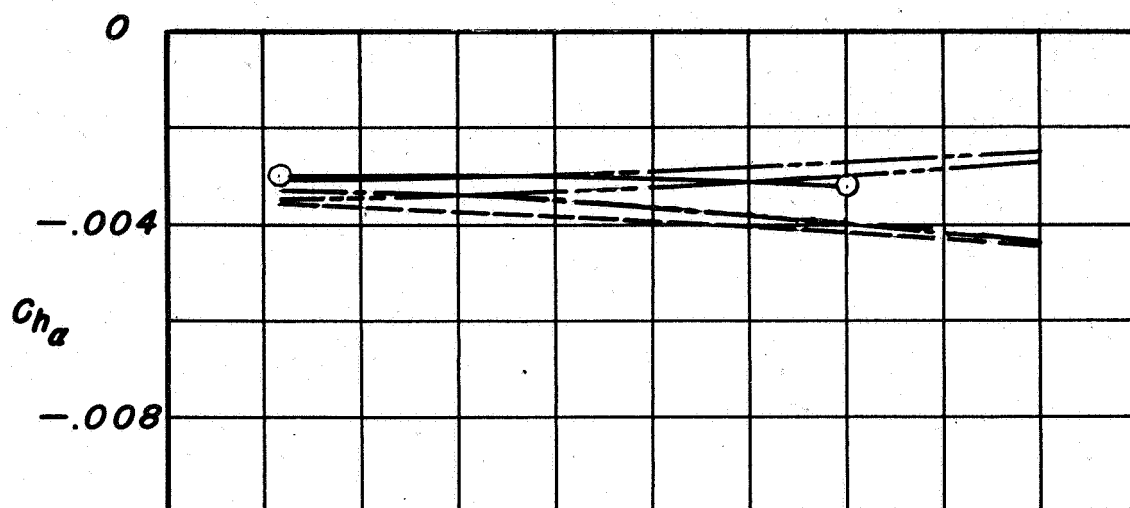


Figure 9.—Comparison of the experimental and calculated lift and hinge-moment parameters as a function of the angle of sweepback. Aspect ratio 6.



(b) Hinge-moment parameters.

Figure 9.—Concluded.

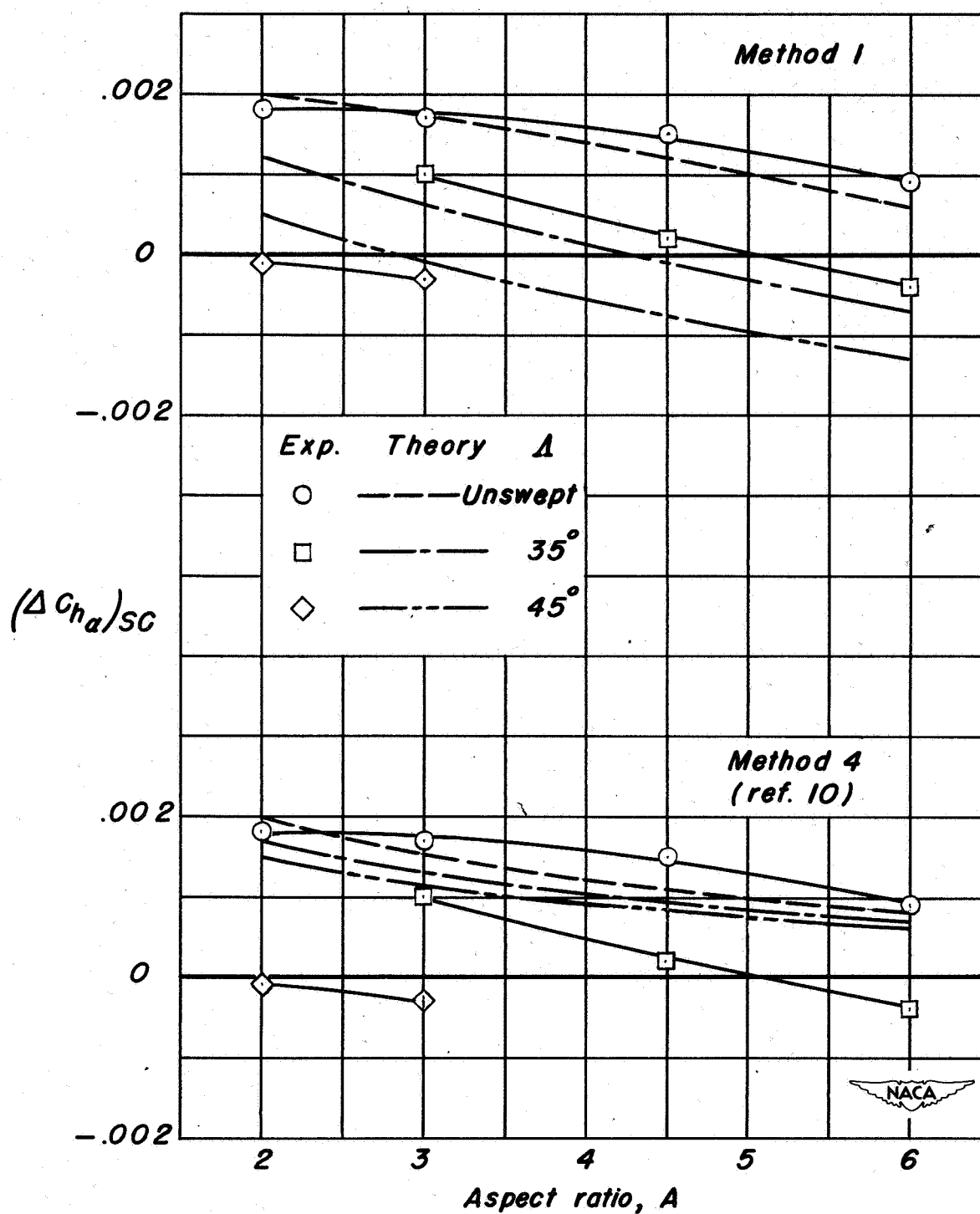


Figure 10.—Comparison of the pseudo-experimental induced-camber correction to C_{ha} with those calculated by Methods 1 and 4.

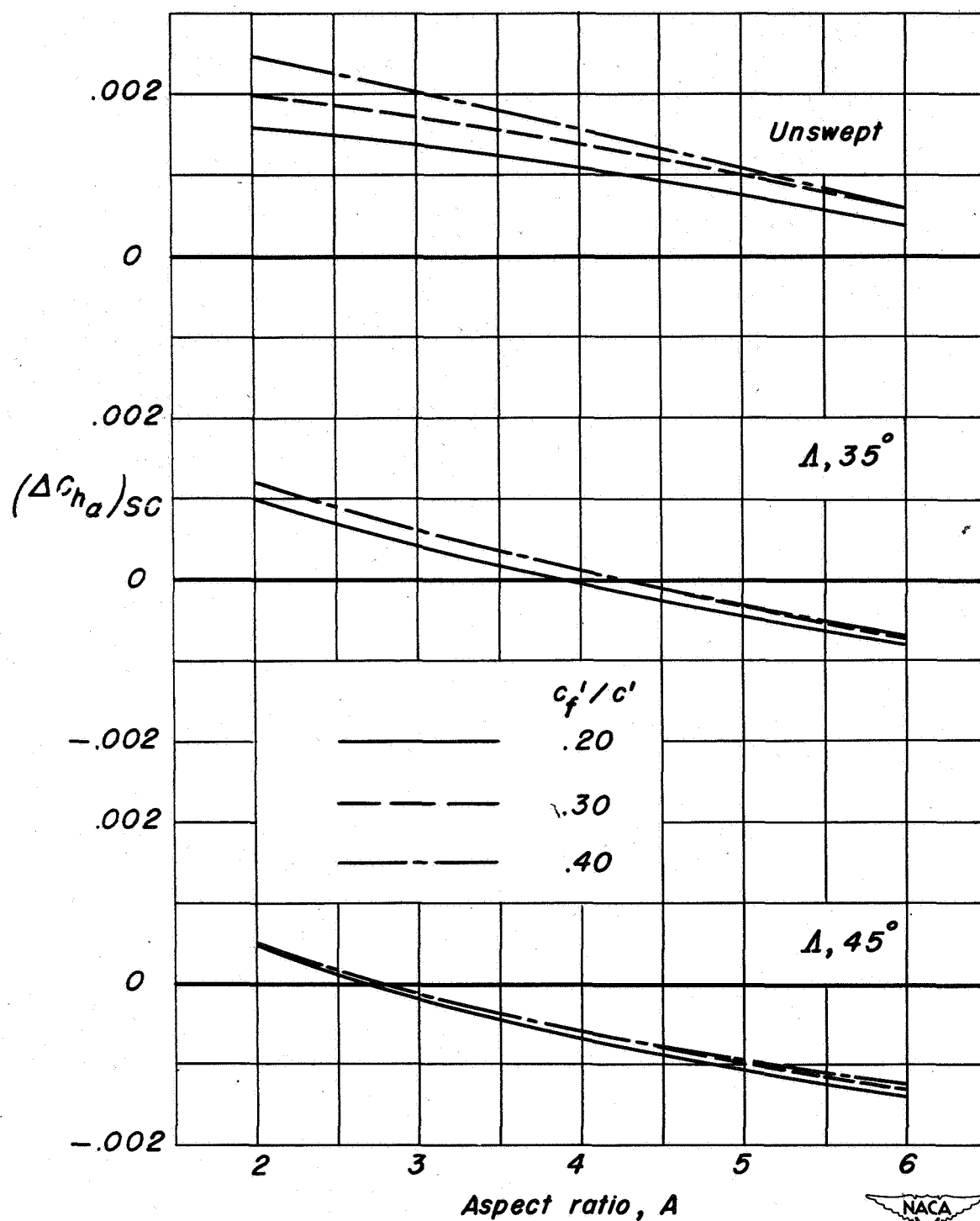


Figure 11.- Induced-camber correction to $C_{h\alpha}$ as a function of the aspect ratio calculated by the Falkner method for use in Method 2.

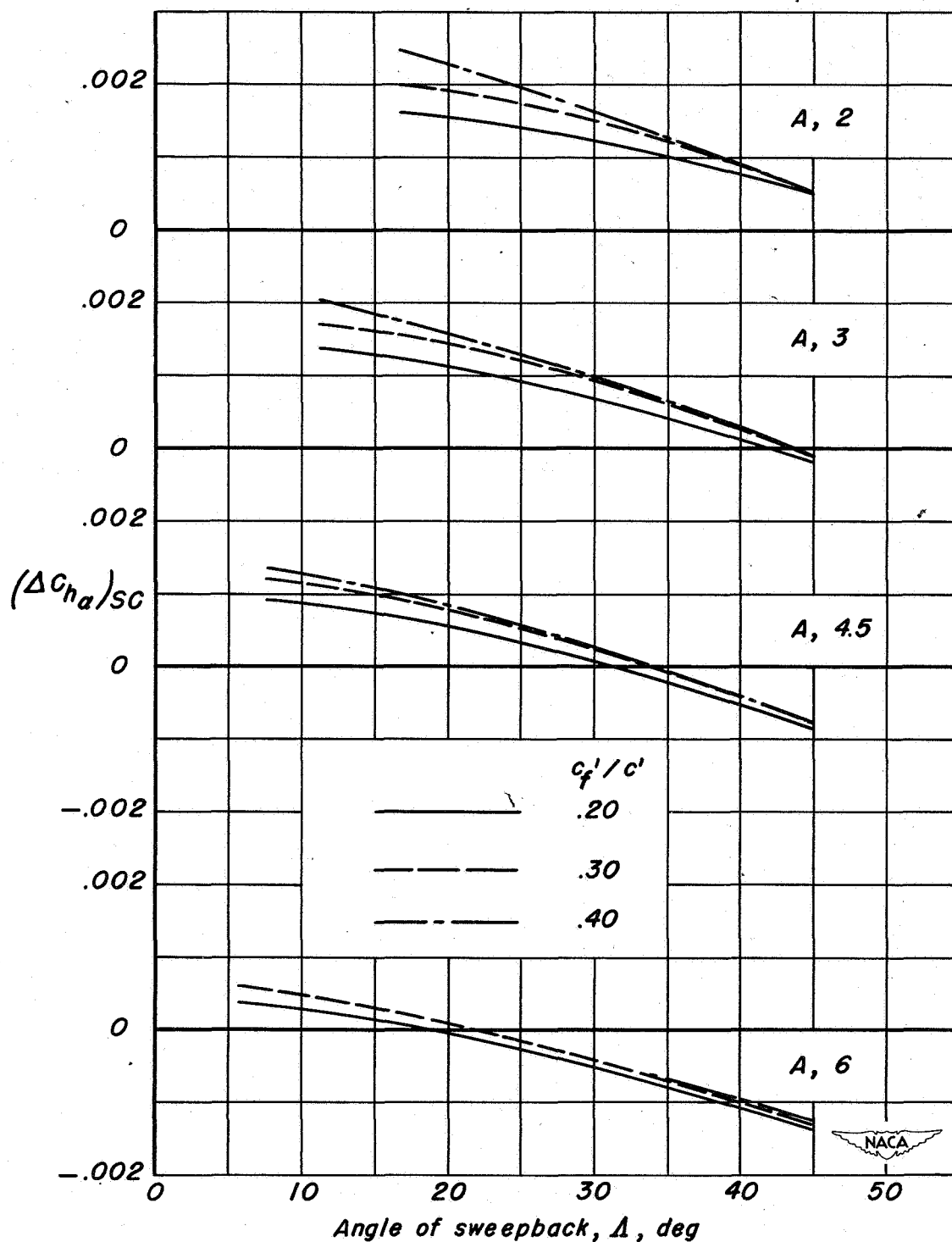


Figure 12.—Induced-camber correction to C_{h_α} as a function of the angle of sweepback calculated by the Falkner method for use in Method 2.